Environment International 158 (2022) 106944

Contents lists available at ScienceDirect

Environment International

journal homepage: www.elsevier.com/locate/envint

Graphene-based materials for the adsorptive removal of uranium in aqueous solutions

Swati Verma, Ki-Hyun Kim *

Department of Civil & Environmental Engineering, Hanyang University, 222 Wangsimni-Ro, Seoul 04763, Korea

ARTICLE INFO

Handling Editor: Guo-ping Sheng

Keywords:
Uranium
Graphene oxide
Adsorption
Partition coefficient
Wastewaters

ABSTRACT

Ground water contamination by radioactive elements has become a critical issue that can pose significant threats to human health. Adsorption is the most promising approach for the removal of radioactive elements owing to its simplicity, effectiveness, and easy operation. Among the plethora of functional adsorbents, graphene oxide and its derivatives are recognized for their excellent potential as adsorbent with the unique 2D structure, high surface area, and intercalated functional groups. To learn more about their practical applicability, the procedures involved in their preparation and functionalization are described with the microscopic removal mechanism by GO functionalities across varying solution pH. The performance of these adsorbents is assessed further in terms of the basic performance metrics such as partition coefficient. Overall, this article is expected to provide valuable insights into the current status of graphene-based adsorbents developed for uranium removal with a guidance for the future directions in this research field.

1. Introduction

Uranium is a silvery-white radioactive element which was first discovered from the mineral called pitchblende in 1789 by a German scientist, Martin Klaproth (Gupta and Walther, 2020). It commonly exists as ^{235}U along with two other isotopic forms of ^{238}U and ^{234}U, where the latter is being produced by the loss of alpha (α) particle from ^{238}U (Krachler et al., 2019). Among these isotopic forms, ^{235}U and ^{238}U are the most radioactive and stable form, respectively (Asic et al., 2017). ^{235}U is the only fissile uranium isotope of which atoms can be split apart through the bombardment of fast energy radioactive particles. Because of its high radioactivity, it is used as an important feedstock to produce nuclear energy in nuclear power plants (Degueldre, 2017). In nuclear power plants, atoms of ^{235}U are attacked by high energy neutrons to split into two lighter weights nuclei (^{92}U and ^{141}Ba) with the emission of three fast energy neutrons through nuclear fission reaction. The emitted neutrons attack other ^{235}U atoms to lead to the nuclear chain reaction. The heat generated during the fission process is consumed to produce steam from water so as to rotate turbine for the production of electrical energy. The same working principle is also applied to the generation of atomic bomb in which uranium is used to induce mass destruction.

Uranium can enter the environment via two channels: anthropogenic and natural routes. Anthropogenic sources of uranium in soil are diverse to include mining of uranium ore from rocks (and its processing) and use of phosphate-based fertilizers (Verma and Dutta, 2015). However, elevated uranium levels in environment is attributed to the unregulated discharge of effluents from nuclear power plants (Tatarchuk et al., 2019). Because of such hazardousness, its maximum permissible concentration in drinking water is regulated such as 30 ppb as recommended by WHO and USEPA (Sar et al., 2018). Inhalation of uranium containing dust or consumption of uranium contaminated water are also considered the common routes of uranium exposure to humans. Potential health hazards associated with the uranium exposure are reported to include lung cancer, kidney cancer, DNA cell damage, and inherited genetic defects. It can also accumulate in the tissues of the central nervous system to affect its functions (Brugge, 2014). In human body, uranium can be coordinated with four to five oxygen atoms if transmitted in the form of carboxylate groups of aspartate, glutamate, water molecules. and other biomolecules (Lin, 2020).

Elevated levels of uranium have been reported from many types of environmental systems, e.g., sediments and ground water areas in Germany (Banning, 2020), well drinking water of Kabul in Afghanistan (Kato et al., 2016), the south-eastern San Joaquin Valley California in USA (Rosen et al., 2019), sheep drinking water in south Africa (Winde et al., 2017), and agricultural soils and drinking water wells on the Swiss Plateau (Bigalke et al., 2018). Consumption of uranium contaminated

* Corresponding author.
E-mail address: kkim61@hanyang.ac.kr (K.-H. Kim).

https://doi.org/10.1016/j.envint.2021.106944
Received 18 June 2021; Received in revised form 19 September 2021; Accepted 17 October 2021
Available online 21 October 2021

water was reported as the main cause of hematological abnormalities (as a proxy for leukemia) in the local people of the Kenhardt municipal district of the Northern Cape Province, South Africa (Winde et al., 2017). Furthermore, grass, tissues, and sheep wool were also identified as alternative sources of uranium exposure to the people of that region. This reflects high uranium contamination in the nearby borehole water with its levels by 20-500 times higher than those of the background concentration. Uranium levels in sheep's wool are higher than those in teeth, bones, and hooves. Conversely, lower amounts of uranium were detected in consumable parts of a sheep's (i.e., meat and inner organs). Also, uranium levels in sheep tissues increased with the age of the sheep. Therefore, removal of uranium from water is essential to reduce health hazards and toxic impacts associated with uranium contamination.

All isotopes of uranium (^{238}U, ^{235}U, and ^{234}U) are subject to a slow rate of disintegration with their half-lives of 4.5 billion, 700 million, and 25 million years, respectively (Baker, 2018). With the half-life nearly equal to the age of earth (~4.54 billion years), ^{238}U is the most abundant isotope of uranium. Consequently, despite the low level of radioactivity, ^{238}U remains as a potent health hazard due to its abundance and lengthy half-life (de Menezes et al., 2020). It mostly exists in + 3, +4, +5, and + 6 oxidation states among which the + 6-oxidation state is most stable in aqueous solutions. The chemistry of uranium in water is interesting in its removal from wastewaters. Uranium (+6) exhibits yellow in color in the form of uranyl ion, i.e., UO_2^{2+} at pH up to 4. At higher pH values (>4), uranyl ions combine with OH^- and CO_3^{2-} ions to turn into diverse ionic species like $[UO_2(OH)]^+$, $[UO_2(OH)_2]$, $[UO_2(OH)_3^-]$, $[UO_2(OH)_4^{2-}]$, $[(UO_2)_3(OH)_5^+]$, $[(UO_2)_3(OH)_7^-]$, $[UO_2CO_3]$, $[UO_2(CO_3)_2]^{2-}$, $[UO_2(CO_3)_3]^{4-}$, and mixed neutral complexes like $(UO_2)_2CO_3(OH)_3$ (Katsoyiannis and Zouboulis, 2013). The relative occurrence patterns of various uranium species in water are shown in Fig. 1.

A number of techniques are used for the removal of uranium ions in aqueous phase (e.g., ion exchange (Amphlett et al., 2020), membrane separation (Ghasemi Torkabad et al., 2017), iron/alum coagulation (Moraes and Ladeira, 2021), lime softening (Courtois et al., 2020), and adsorption (Gao et al., 2014)). Among these options, adsorption is the most widely adopted option for reducing uranium levels in water owing to its simplicity, easy operation, effectiveness, and low-cost features. Moreover, mechanistic aspects of adsorption process can be easily analyzed with the aid of various adsorption (isotherms and kinetic) models as commonly reported in the literature. (Ayawei et al., 2017; Pal, 2017). The details on the adsorption mechanism further help in optimizing reaction conditions to achieve best performance. A plethora of absorbents (synthetic/natural polymers, inorganic materials, clays, etc.) have been developed for uranium removal and showed great performances. Polymers-based adsorbent materials possess diverse functional

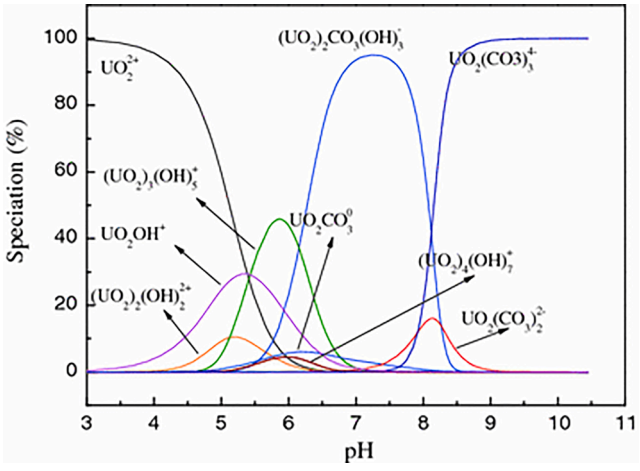

Fig. 1. Distribution profiles of uranium (VI) species at different pH values (Zhang et al., 2011).

groups, which can be modified to achieve selective and rapid adsorption of uranium. Likewise, many inorganic materials including silica, alumina, titania, and iron (III) oxide were found to be potential adsorbents for uranium due to their high surface area, porosity, and tunable pore characteristics (Jo et al., 2018; Wang et al., 2018a; Tatarchuk et al., 2019; Ahmad et al., 2020; Singhal et al., 2020).

Among numerous adsorbents explored for uranium removal, the potential of both conventional and modernized forms of carbon-based materials is recognized to be remarkable owing to their greenness and cost-effectiveness (Guo et al., 2021). Activated carbon (AC) is the most used carbon adsorbent employed for environmental remediation applications such as removal of toxic heavy metals and dissolved organic pollutants (e.g., dyes, pharmaceutical, and organics) from aqueous systems (Gopinath et al., 2021). The role of AC materials in the abatement of radioactive elements is also recognized to be outstanding. A recent study reported enhanced removal efficiencies of wood waste-derived AC against thorium (87.96%) and uranium (97.94%) ions from acidic solutions. (Alahabadi et al., 2020). The effectiveness of wood wastes derived AC was ascribed to the existence of micro-size transitional pores which facilitated uranium removal via constrained diffusion mechanism. Similarly, AC obtained from other waste materials such as tires, carbon powder waste, sawdust powder, and waste areca residue were also utilized successfully for uranium removal application (Belgacem et al., 2014; El-Magied et al., 2017; Wua et al., 2020; Nezhad et al., 2021). Activated charcoal is also a kind of AC which was also used for uranium removal (Liu et al., 2016a; Wang et al., 2021b). Advanced carbon materials such as carbon quantum dots, carbon nanotubes (CNTs), and graphene oxide have also been recognized as alternate carbon materials for metal removal to replace conventional AC materials (Abdeen and Akl, 2015; Wu et al., 2018; Mahmoud et al., 2020; Liu and Mao, 2021). Among them, graphene oxide (and its derivates like reduced graphene oxide, functionalized graphene oxide, and graphene oxide composites) have emerged as superior adsorbents for uranium owing to its unique 2D network structure and surface functional groups (Fig. 2). For example, graphene oxide recorded higher copper removal efficiencies of 75% at pH 5.5 in comparison to AC (36%) and carbon nanotubes (~15%) (Ren et al., 2013). Higher performance of GO over AC and CNTs was attributed to its higher abundance of oxygen moieties and higher BET surface area. Further, the uranium adsorption capacity of activated carbon felt (ACF) was reported to increase from 173 mg/g to 298 mg/g by forming GO-ACF composite with the aid of hydrophilicity induced by GO and its functional groups (Chen et al., 2013). The suitability of other graphene-based adsorbents for uranium removal was also addressed (Xiao et al., 2016; Kumar et al., 2017). Therefore, it can be inferred that graphene-based adsorbents are superior to traditional AC and modern CNTs materials in removing U species because of their unique surface related characteristics.

In this review, the basic features of graphene-based materials are explored with respect to their applications toward the environmental remediation. Brief discussions are made on the protocols of GO synthesis and associated modification strategies based on their categorization in relation to chemical compositions. Performances of different graphene adsorbents have also been evaluated in terms of the key performance metrics such as adsorption capacity and partition coefficient (Vikrant and Kim, 2019). The key role of functional groups and other components in promoting uranium removal has been discussed in relation to experimental conditions and material characteristics.

2. Graphene in water remediation processes

Graphene and its composites have been extensively studied as advanced adsorbents for the removal of organic pollutants from wastewater (Kumar et al., 2017). Its excellent performance in adsorption applications is ascribed to its physio-chemical characteristics such as layered 3-D structure, large theoretical surface area, highly conjugated network of fused aromatic rings, presence of diverse functional groups

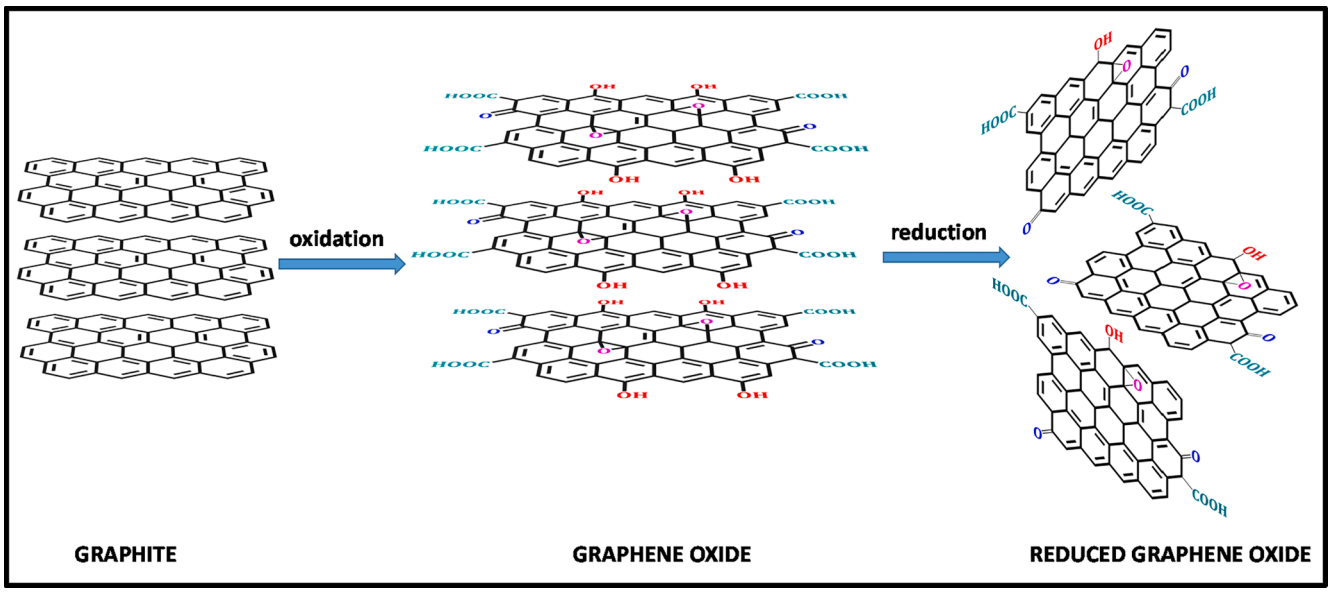

Fig. 2. Structures of graphite, graphene oxide, and reduced graphene oxide.

on its surface, and its high thermal–mechanical stability (Ersan et al., 2017; Lai et al., 2019; Wang et al., 2020b). Removal of cationic and anionic dyes by graphene-based adsorbents is facilitated by hydrophobic π-π interactions, hydrogen bonding, and electrostatic interactions (Kim et al., 2015). Graphene was also explored as a 2-D support material for loading semiconductor photocatalyst materials. Synergistic effects between graphene sheets and metal oxide nanoparticles help in achieving higher photocatalytic efficiency and impart mechanical strength to the photocatalyst material (Wang et al., 2018b). Graphene-based photocatalysts composites show enhanced photocatalysis due to transportation of photogenerated electron at the graphene-metal oxide heterojunction (Upadhyay et al., 2014). This process eventually suppresses electron/hole recombination process and boosts production of reactive oxygen species that prompts degradation/mineralization of organic pollutants. The difference in the nature of chemical interactions that causes removal of dyes by commercial graphene and graphene oxide is shown in Fig. 3.

In addition to the removal of organic pollutants, graphene-based adsorbents have also been studied extensively as adsorbents for toxic heavy metal impurities present in wastewater (Pérez-Ramírez et al., 2016). Different types of chemical interactions that facilitates removal of toxic uranium ions by graphene, graphene oxide, and reduced graphene oxide is shown in Fig. 4. As can be seen, introduction of oxygen functional groups in GO and rGO induces electrostatic interactions and thus lead to effective removal of uranium ions. Likewise, removal of Cu (II) ions by GO was studied by varying operational parameters that affect adsorption (Wu et al., 2013). Accordingly, surface oxygen moieties are responsible for the abstraction of Cu(II) ions from an aqueous medium. A maximum adsorption capacity of 117.5 mg/g at pH 5.3 over a contact time of 150 min was achieved using a 1.0 mg/mL GO adsorbent dose. The spent GO adsorbent can easily be regenerated by washing with dilute HCl and retains >90% of its initial adsorption capacity after ten consecutive adsorption cycles. GO was also found to be appropriate for the removal of other toxic metal ions such as nickel, gold, cadmium, zinc, lead, platinum, cobalt, and antimony (Peng et al., 2017).

Apart from heavy metals, the potency of graphene oxide was also examined against radioactive elements of the actinide series, i.e., thorium, uranium, neptunium, plutonium, and americium along with

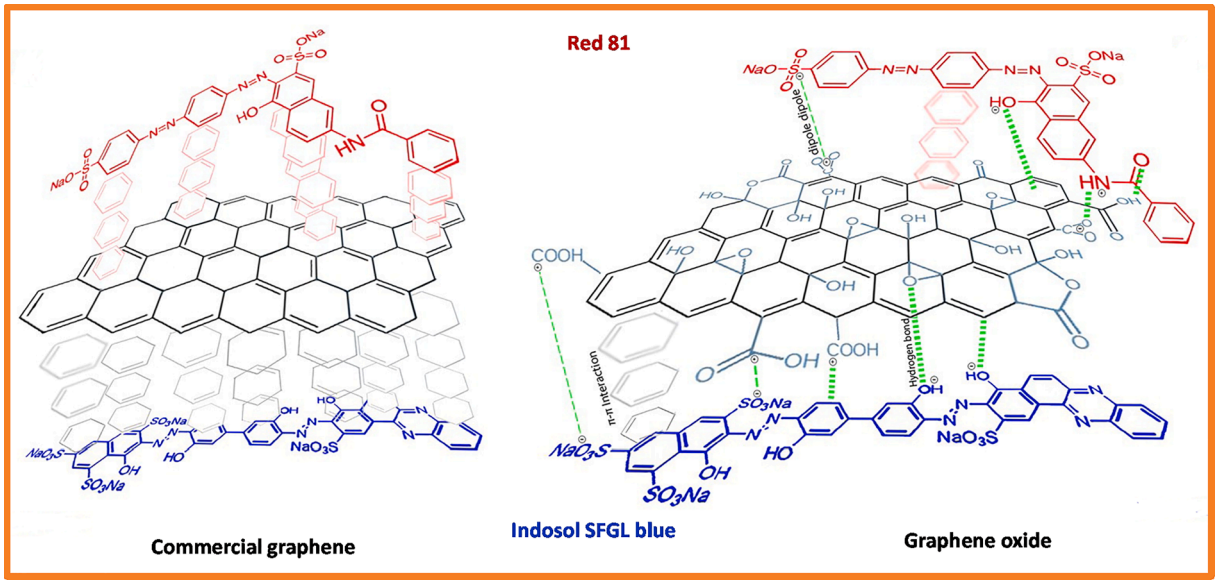

Fig. 3. Different chemical interactions involved in the adsorption of dyes by graphene and graphene oxide (de Assis et al., 2020).

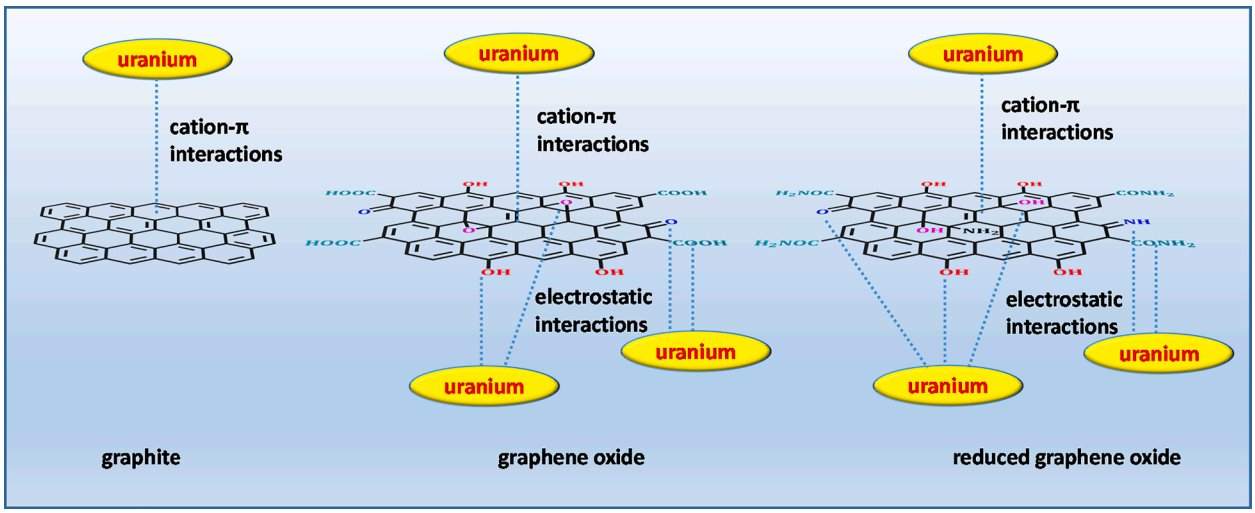

Fig. 4. Possible chemical interactions of graphite, graphene oxide and reduced graphene oxide (by amination) with uranium.

their fission products, i.e., strontium, europium, and technetium (Romanchuk et al., 2013). It was observed that the hydrophilic GO sheets coagulate upon interaction with metal ions to form metal-GO aggregates, which could be then readily separated by filtration or centrifugation. The effectiveness of GO in the removal of said radionuclides was also examined in the presence of common cations (e.g., Na and Ca) and anions (e.g., sulphate, carbonate, citrate, and acetate) that are generally present in liquid nuclear wastes. Accordingly, GO exhibits high adsorption capacities and selectivities against all targeted radionucleotides even in the presence of common ionic impurities. GO exhibits high uranium removal of ~ 70% at pH 7.5 despite the formation of stable anionic species in solution with pH of above 4. (Romanchuk et al., 2013). On the other hand, conventional adsorbents such as granular AC and bentonite clay recorded lower U removals of 10% and 40%, respectively, at the same pH of 7.5. This implies that graphene-based adsorbents are also suitable for the adsorption of anionic U species at high pH values. Few other studies also demonstrate the utility of GO-based adsorbents toward the removal of radionucleotides such as uranium, europium, cesium, and strontium from aqueous solutions (Wang et al., 2015b; Wang et al., 2016b). Hence, it can be concluded that GO and its derivatives are promising materials for environmental remediation due to their enhanced ability to incorporate diverse functional groups on the unique 2-D layered structure.

3. Protocols for GO synthesis

In the past decade, graphene and its diverse derivatized forms have received global attention in environmental remediation processes such as removal of toxic organic pollutants and metal ions from wastewater (Yu et al., 2015). The suitability of graphene-based materials in environmental remediation is ascribed to its amazing 2-D aromatic skeleton, which is composed of sp^2-hybridized carbon atoms (Allen et al., 2010). Another striking features of graphene is its large theoretical surface area of 2630 m^2/g, which makes it an excellent candidate for adsorption processes (Yu et al., 2015). However, graphene in its native form exhibits hydrophobicity due to the absence of polar functional groups. This restricts the interactions between pure graphene sheets and organic or inorganic pollutant compounds, and thus restricts its application in adsorption processes (Chabot et al., 2014). Hence, functionalization of graphene is the key means of inducing adsorptive properties in graphene sheets. The most common way of functionalizing graphene is to perform a chemical oxidation to obtain graphene oxide (GO) using Hummers' method (Hummers Jr and Offeman, 1958). In Hummer's method, graphite powder or flakes are treated with a mixture of $NaNO_3$ and $KMnO_4$ in H_2SO_4 to produce GO. The process of graphene oxidation is facilitated by the *in-situ* formation of dimanganese heptoxide, i.e., Mn_2O_7 (Eq. (1) & (2)), from the reaction between H_2SO_4 and $KMnO_4$ (Kumar and Srivastava, 2018). This Mn_2O_7 species readily diffuses through graphene layers to form manganese esters at the defective centers present within the graphene sheets (Eigler and Hirsch, 2014). Consequently, GO is obtained upon the hydrolysis of manganese esters by water and subsequent solubilization of manganese-oxo species by hydrogen peroxide. Later, modifications and improvements were accomplished in the well-known Hummer's method to achieve GO sheets with high oxygen content (Marcano et al., 2010). These modification strategies include usage of $NaNO_3$ in higher amounts (as compared to Hummer's method) and its replacement by H_3PO_4 to achieve a higher concentration of oxygen containing functional groups.

$$KMnO_4 + H_2SO_4 \rightarrow K^+ + MnO_3^+ + H_3O^+ + 3HSO_4^- \quad (1)$$

$$MnO_4^- + MnO_3^+ \rightarrow Mn_2O_7 \quad (2)$$

The structural elucidation of GO is a subject of great interest due to the limited information on the oxidation mechanism of graphene sheets. Insights of oxidation mechanism is essential to describe the introduction of various oxygen moieties in the graphene skeleton (e.g., hydroxyl, carbonyl, epoxy, and carboxylic acid). It is assumed that the large and conjugated network of graphene has many structural defects at the edges and basal planes. Such defect points serve as the active centers for the approaching oxygen functional groups to initiate the oxidation process. In the Hummer's oxidation process, hydroxyl (–OH) and carboxylic acid (–COOH) groups are formed at the edges and in the basal plane of graphene sheets. As the reaction progresses, epoxy groups are generated with the loss of water molecules from adjacent hydroxyl groups. Based on the above assumptions, the structure of GO containing carboxylic acid groups (at the edges) and hydroxyl/epoxy groups at the basal plane is shown in Fig. 2 (Nasrollahzadeh et al., 2015). The total amount of oxygen containing functional groups in GO is generally expressed as total oxygen content. Higher oxygen content in GO implies a higher degree of oxidation of graphene sheets.

In the recent years, electrochemical method has emerged as a green approach for GO synthesis (Pei et al., 2018). Electrochemical method is regarded as green, cost-effective, and fast approach with the following advantages: (i) no requirement for strong oxidizing agents, (ii) suitability for large-scale GO production due to relatively shorter reaction periods, and (iii) production of high-quality graphene sheets with high oxidation contents. This technique makes use of non-toxic electrolytes

for the exfoliation of graphene sheets from cheap precursor materials like graphite electrode, pencil lead, and graphite paper. The insertion of ionic moieties into graphene sheets not only causes graphene exfoliation but also offers oxygen moieties (Liu et al., 2013). (Fang et al., 2019). Some efforts have also been made to couple the Hummer's oxidation method with electrochemical approach to achieve higher oxidation levels in GO (Kumar and Srivastava, 2018).

4. Modification strategies for GO

4.1. Heteroatom addition

Reduced graphene oxide (rGO) is the most promising derivative of graphene as it found huge applicability in environmental remediation processes due to reduced hydrophilicity. rGO can be considered as one of the derivatives of GO in which some of the oxygen containing functional groups are removed or modified to re-establish the conjugated network of graphene. There are various ways of producing rGO from GO such as thermal annealing, solvothermal, chemical, and electrochemical methods (Pei and Cheng, 2012). In the thermal reduction method, GO is annealed at high temperatures and under inert conditions mostly. Thermal annealing enables loss of oxygen functional groups (i.e., –COOH groups) as CO_2 and intercalated water molecules as water vapors and thereby create huge pressure to separate out stacked GO sheets (Tu et al., 2015; Saleem et al., 2018). Solvothermal reduction of GO was achieved by heating a dispersion of GO in organic solvents (including water) at the boiling point of the solvent in use. Here, alcohols, ethylene glycol, dimethyl formamide (DMF), and N-methyl-2-pyrrolidinone (NMP) are used as common solvents to induce the solvothermal reduction of GO (Park et al., 2009; Dubin et al., 2010; Seo et al., 2013). These solvents have dehydrating properties and thus they produce rGO via removal of attached functional moieties as water molecules. Similarly, GO reduction could also be achieved using electrochemical and photoreduction techniques using electrons and photons as activation mediators, respectively.

Chemical functionalization of GO via covalent and non-covalent approaches is the most used strategy for producing functionalized GO sheets (Chua and Pumera, 2014). Chemical functionalization of GO with reducing agents containing heteroatom(s) (e.g., nitrogen (N), sulfur (S), and phosphorous (P)) resulted in the doping of the GO lattice with the constituting atom (Kumar and Khandelwal, 2014; Wu et al., 2019; Fan et al., 2020; Kumar and Srivastava, 2021). Here, it is worth shedding light on the significant role of organic chemistry in facilitating the modification of GO. Organic chemical reactions such as amination, esterification, and diazonium salt formation are reported to play a major role in modifying oxygen moieties and native C = C bonds of GO (Kasprzak et al., 2018). Briefly, –COOH groups existing at GO edges can be easily derivatized through nucleophilic substitution reaction to yield graphene derivatives with amine or amide functionalities (Valeur and Bradley, 2009). Likewise, epoxy rings of GO structure can be modified by triggering a nucleophile attack on the sp^3 carbon atom (Georgakilas et al., 2012). In an another attempt, room temperature treatment of GO with NH_3 gas modified its native structure by introducing amide and amine groups at the surface (Yeh et al., 2013). This kind of modification imparts n-type conductivity to GO sheets to help facilitate photocatalytic splitting of water molecules to produce hydrogen and oxygen. Similarly, hydrothermal treatment of GO with hydrazine causes GO doping with aromatic nitrogen by generating a pyrazole ring at the edges of the graphene skeleton (Park et al., 2012). An S-doped GO sponge was prepared by the thermal treatment of GO nanosheets with sulfur powder in inert conditions and was used as a free standing electrode for potassium-ion (K-ion) batteries (Li et al., 2018). The improved electrochemical performance of S-doped GO as compared to undoped GO is ascribed to its conductive structure, which is effective in restricting K-ion migration. Improved NH_3 sensing properties at room temperature were achieved by thermally annealing a mixture of GO with triphenyl phosphine (Niu et al., 2014). Thus, it can be concluded that chemical functionalization and simultaneous doping of GO with heteroatoms are a useful option to improve the performance of the resulting material by imparting active sites for various applications.

4.2. Composite formation

Several types of GO composites were prepared by adding metal oxide nanostructures and other miscellaneous material to the layered material. In this regard, GO is combined with conventional inorganic adsorbent materials such as silica (GO/SiO_2) and alumina (GO/Al_2O_3) (Meng et al., 2015; Zhang et al., 2019a). Synthesis of GO/SiO_2 composite was obtained using a sol–gel technique, whereas GO/Al_2O_3 composites were derived by simple physical mixing of mesoporous alumina with GO dispersion. The nature of constituting metal ions imparts different adsorption characteristics to GO to enable uranium removal at different pH conditions such as pH 4 by GO/SiO_2 and pH 6 by GO/Al_2O_3 composites. Transition metal oxides are a well-known component for composite formation due to their remarkable characteristics in various energy and environmental applications. However, their instability under acidic conditions restricts their application in several processes (Huynh et al., 2017). To overcome such drawback, 3-dimentional graphene oxide/titanium oxide (3D GA/TiO_2) composites were prepared by one-step hydrothermal approach (Yu et al., 2019). Briefly, GO and Ti precursors are added in DI water and simultaneously precipitated out at 180 °C using ammonia to form hybrid material. The incorporation of GO sheets was found to improve chemical stability of TiO_2 for effective removal of uranium ions under acidic conditions.

As are the cases of metal oxides, GO sheets were also used to impart the stability of MOFs in solutions for the enhanced uranium removal efficiency. As an example, GO-MIL-(1 0 1)Fe composite with various graphene content was developed using in-situ growth method (Han et al., 2018). It has been observed that the incorporation of GO sheets in MIL MIL-(1 0 1)Fe MOF reduced its surface area from 537.98 to 246.56 m^2/g, while improving its adsorption performance with the aid of complex surface chemistry. GO is also combined with other materials and tested for uranium removal. For instance, GO composite formed with clay materials exhibited the great potential in metal removal applications owing to large surface area and cation-exchange properties. Graphene oxide/bentonite composites were prepared using simple mixing method for the removal of uranium ions in wide pH range of 2–10 (Liu et al., 2018a). Incorporation of bentonite clay particles in between GO sheets not only enhanced its adsorption capacity by restricting agglomeration of GO sheets but also facilitated its separation through membrane filters. GO composites with biopolymers were also developed in an effort to develop efficient adsorbent materials for uranium. Biopolymers such as chitosan (CS), bovine serum albumin (BSA), and sodium carboxymethyl cellulose (CMC) contain a large number of oxygen and nitrogen moieties to effectively uptake uranium through diverse interactions (Huang et al., 2017; Peng et al., 2019). Fabrication of GO composites with CS, BSA, and CMC biopolymers was achieved by ultrasonication method (for the prevention of agglomeration). Likewise, many other synthesis methods were also proposed for preparing GO composites for uranium removal applications.

5. Emergence of graphene-based adsorbent for uranium

Research on the adsorption of U(VI) ions by graphene-based adsorbent was first reported in 2012 (Zhao et al., 2012). These authors prepared a few-layered graphene oxide adsorbent from graphite precursor using a modified Hummer's method. The zero-point charge (pH_{ZPC}) of the prepared few-layered GO nanosheets was 3.89, indicating that the GO surface can take positive and negative charge below and above this pH, respectively. Further investigations of U ions adsorption on GO indicates that the adsorption process is strictly pH dependent with a maximum adsorption capacity (i.e., q_{max}) of 97.5 mg/g at pH 5 ± 0.1. As

uranium complexes with OH– ions and forms negative species at pH values > 5, their adsorption on a negatively charged surface of GO becomes unfavorable. Conversely, GO absorbs H^+ ions from aqueous medium to discourage the adsorption of U ions on its surface at low pH values < 5. Also, it was observed that U adsorption is independent of the ionic strength of the medium but occurs mainly at the surface oxygen functional groups via inner-sphere surface complexation. The suitability of a Langmuir adsorption isotherm model suggests that monolayer coverage of U ions may take place dominantly on the GO surface (Zhao et al., 2012). Later, several studies were published on the usefulness of GO as an adsorbent for U ion removal (Wang et al., 2015a; Wang et al., 2015b). Some of those studies reported significantly higher U adsorption capacity values like 138. 9 mg/g (Sun et al., 2015a), 142.3 mg/g (Mohamud et al., 2018), 257.2 mg/g (Wang et al., 2016c), 299.0 mg/g (Li et al., 2012), and 299.7 mg/g (Li et al., 2019), than that discussed above. A large variation in the uranium adsorption capacity values by diverse GO adsorbents could be ascribed to the combined effects of various factors such as different C/O ratio of these GO materials and adsorption experimental conditions.

Later, the functional groups of graphene-based materials were modified as a favorable approach to improve their adsorption performance towards U ions. In this context, oxygen containing functional groups of GO were modified with nitrogen containing chemical agents such as ammonia (Verma and Dutta, 2015), polydopamine (Zhao et al., 2015), polypyrrole (Hu et al., 2014), ethylenediamine tetra acetic acid (EDTA) (Liu et al., 2017), and polyaniline (Sun et al., 2013). These chemical compounds provide $–NH_2$ functional moieties on the surface of GO nanosheets to improve the affinity for U ions on the GO surface. The adsorption capacities values corresponding to the above moieties have been determined to be good (80.1, 145.4, 147.1, 212.8, and 245.1 mg/g, respectively). Polyethyleneimine (PEI) is an important amine-containing polymer that can significantly improve the U adsorption capacity of GO. Three different studies were reported on U removal using PEI modified GO adsorbents, i.e., GO-pDA-PEI (Li et al., 2019), GO-PEI (Huang et al., 2018), and PEI-GHS adsorbents (Wang et al., 2017). They all exhibited very high q_{max} values of 416, 629.5, and 989 mg/g, respectively. Similarly, the GO surface was also modified with phosphate (PO_4^{2-}) containing chemical compounds, such as phytic acid (q_{max} = 483 mg/g) (Cai et al., 2019) and triethyl phosphite (q_{max} = 251.7 mg/g) (Liu et al., 2015b) to enhance U ion removal. In a few studies, the sulfate (SO_4^{2-}) functionalization of GO was also reported for the adsorption of U ions from aqueous media (Zhang et al., 2016; Sun et al., 2017). Functionalization of GO with biomolecules led to the introduction of diverse types of functional groups on GO surfaces. In this regard, GO bound with L-cysteine amide (Verma and Dutta, 2017) and adenosine 5′-monophosphate (Dutta et al., 2019) yielded adsorption capacity values of 176 and 186.2 mg/g, respectively. Therefore, it can be inferred that the use of functional groups such as $–NH_2$, $-PO_4^{2-}$, and $-SO_4^{2-}$ should be an effective option to improve the adsorption performance of GO against U ions.

Graphene oxide and its modified forms exhibit excellent adsorption capacity toward U due to the presence of various polar functional groups on its surface. At the same time, polar functional groups impart hydrophilicity to GO nanosheets and make post treatment separation of GO nanosheets laborious (Khan et al., 2019). To overcome this drawback, magnetic components were introduced into graphene-based adsorbents to allow facile post separation of the used adsorbent. The magnetic component in the GO adsorbent was introduced in diverse forms such as Fe_3O_4 (Zong et al., 2013), $CoFe_2O_4$ (Tan et al., 2015a), and $NiFe_2O_4$ (Lingamdinne et al., 2017) to allow easy adsorbent recovery. For example, GO nanosheets prepared using Hummer's method exhibited a q_{max} value of 60.6 mg/g at pH 3.5 for a contact time of 3 h (Lingamdinne et al., 2017). Under similar experimental conditions, GO- $NiFe_2O_4$ (GONF) composites showed much improved q_{max} value of 135.1 mg/g, suggesting that the oxygen of nickel ferrite also participates in the process of U adsorption along with the oxygen functional groups of GO. An enhanced adsorption capacity of 200 mg/g was achieved when GONF was reduced to rGONF nanocomposites using hydrazine as a reducing agent. This is because hydrazine functionalization provides nitrogen containing functional groups on GO surface to upgrade its affinity for U ions. Considering the role of magnetic nanoparticles and nitrogen containing functional groups in the removal of U ions, efforts were made to develop ternary amidoximated magnetite/graphene oxide (AOMGO) (Zhao et al., 2013), polyamidoxime/polyethyleneimine magnetic graphene oxide (mGO-PP) (Dai et al., 2019a), and polyamidoxime functionalized magnetic graphene oxide (mGO-PAO) (Dai et al., 2018). The corresponding q_{max} values were 294.7, 200.4, and 89.9 mg/g, respectively. Additionally, GO composites with TiO_2 and MnO_2 were also developed to show high adsorption capacity values of 441.3 and 153.9 mg/g, respectively (Yang et al., 2018; Yu et al., 2019). The approach of adding magnetic nanoparticles was also useful in case of uranium removal via photocatalytic mechanism (Li et al., 2017).

Miscellaneous types of GO adsorbents were also developed which revealed excellent adsorption capacity values towards U adsorption. For example, reduced graphene oxide-zeolitic imidazole framework-67 (rGO/ZIF-67) hydrogel showed an extremely high U adsorption capacity of 1888.55 mg/g at pH 4.01 (Zhao et al., 2020). Similarly, GO gels with polyvinyl alcohol/sodium alginate (SPG) (Yi et al., 2018), carboxymethyl cellulose/3-aminopropyltriethoxysilane (GO-CMC-AO) (Yang et al., 2020), chitosan/3-aminopropyltriethoxysilane (GO-CS-AO) (Yang et al., 2020), bovine serum albumin (GO-BSA) (Yang et al., 2017), and polydopamine/chitosan (GO@PDA/CS) (Liao et al., 2018) showed high q_{max} values of 403.8, 307, 243.4, 270, and 161 mg/g for U removal from aqueous solution. The amazing adsorption capacity values of GO-based gel adsorbents were attributed to their porous structure network and presence of diverse functional moieties.

6. Uranium adsorption mechanism

Uranium adsorption on the surface of heterogenous adsorbents is significantly influenced by the pH of the solution. As the dominant forms of U species vary across varying pH conditions, their adsorption is highly susceptible to pH change. It can be seen that 95% of U exists in the form of cationic UO_2^{2+} species along with 5% as $UO_2(OH)^+$ and $(UO_2)_2(OH)_2^{2+}$ at pH < 4 (Fig. 1). In the pH range of 4 to 8, $(UO_2)_3(OH)_5^+$ is the most dominant followed by $(UO_2)_4(OH)_7^+$. Above pH 8 and 9, $(UO_2)_3(OH)_7^-$ and $UO_2(OH)_3^-$ are the dominant species, respectively. In contrast to this, GO bearing oxygen moieties possesses a negative surface charge in the pH range of 2–9, making GO and its composites an excellent adsorbent for the cationic metal impurities including uranium (Verma and Dutta, 2015). However, the magnitude and nature of the surface charge of GO can increase or decrease depending on the pH and on strategies used for the modification of its surface as shown in Fig. 5(a & b) (Konkena and Vasudevan, 2012; Verma and Dutta, 2017). However, in most cases, GO-based adsorbents carry negative surface charge and are thus able to facilitate the removal of heavy metal ions by electrostatic interactions. As an example, pure GO adsorbent enhanced removal efficiencies from 50% to 66% with an increase in solution pH from 2 to 11 (Wang et al., 2020a). This is because the surface of GO adsorbents is characterized by negatively charged active binding sites, which can abstract H^+ ions from aqueous solution to lower the removal efficiency at low pH values. In contrast, adsorption of H^+ ions from solution to the GO surface decreases with increasing pH to stimulate the adsorption of U. On the other hand, CTAB modified GO (MGO) showed a noticeable effect of pH in the removal of U from 50% (at pH 2.0) to nearly 99% (at neutral pH 7.0) (Wang et al., 2020a). This can be attributed to the favorable electrostatic interactions that prevail between cationic U species and the negatively charged surface of MGO. At pH > 7, a slight decrease in the removal efficiency was observed due to the formation of anionic U species. Nonetheless, the overall effectiveness of the process is above 90%, implying high relevancy of MGO adsorbent towards U removal.

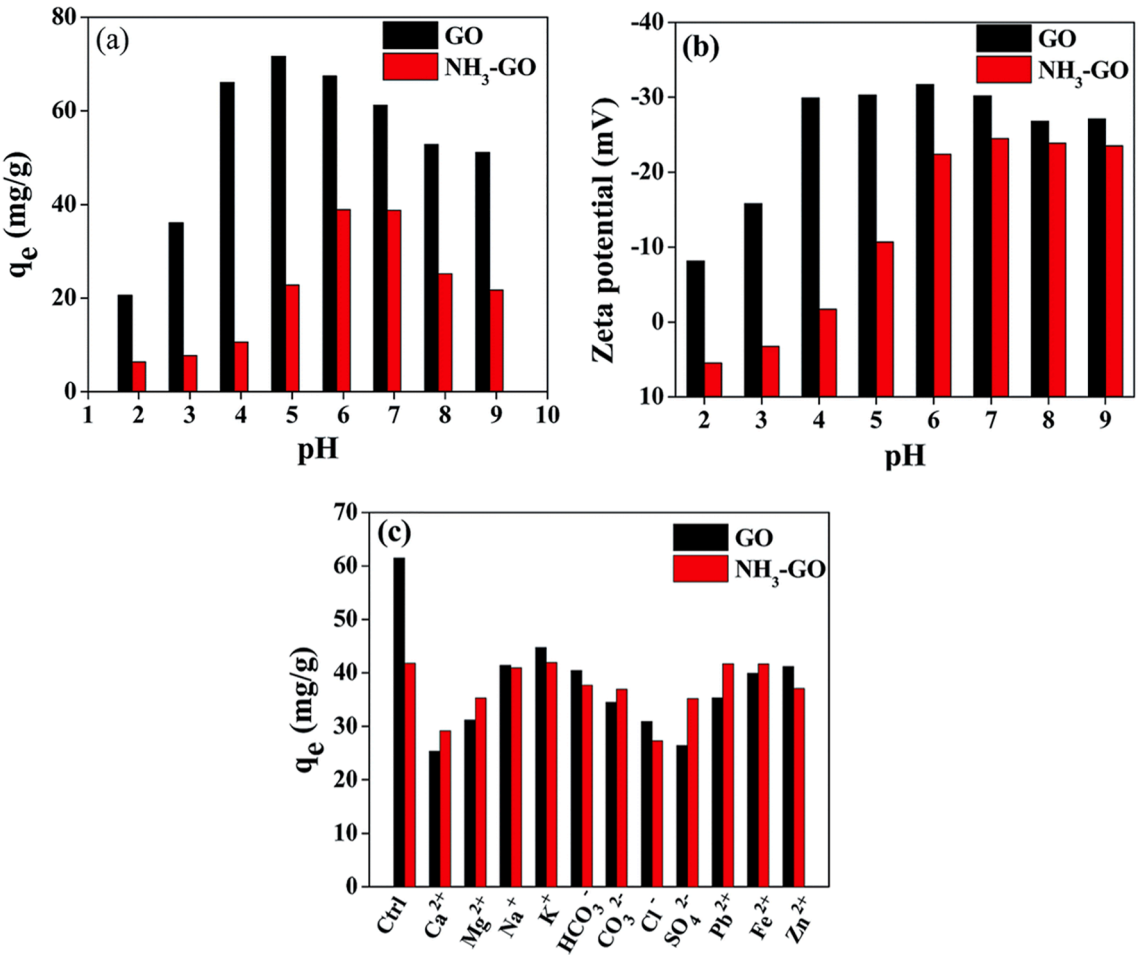

Fig. 5. Factors affecting U adsorption on GO and NH_3GO adsorbents: (a) Effect of pH on q_e values of uranium ion adsorption on GO and NH_3-GO, (b) effect of pH on zeta potential of GO and NH_3-GO, and (c) effect of interfering ions on uranium ions adsorption by GO and NH_3-GO (Verma and Dutta, 2015).

Relatively low adsorption of U in the low pH range may reflect the competitive nature of H^+ ions from solution which hindered or suppressed the adsorption of U species on the surface of MGO adsorbent. Similar observations were made in U adsorption by graphene oxide-activation carbon felt (GO-ACF) composites with a maximum adsorption achieved at pH 5.3 (Chen et al., 2013). This is ascribed to the existence of anionic U species at pH above 5.3, while adsorption of H^+ ions on the GO-ACF surface is promoted below pH 5.3.

Variation in solution pH also affects the mechanism of adsorbent and U interactions. For example, a multifunctional graphene oxide-chitosan (GO-CS) hydrogel is reported to be very good at removing U species from solution over a wide pH rage of 3.5–8.3 (Huang et al., 2017). Its adsorption capacity values observed at pH 3.5, 5.0, and 8.3 were 200, 319.9, and 384.6 mg/g, respectively. It was concluded that surface complexation of U species was facilitated by the active sites anchored as –COOH, –OH, and $–NH_2$ functional groups at pH 3.5 and 5.0. In contrast, U adsorption at pH 8.3 is mainly driven by $–NH_2$ moieties present on chitosan molecule, which eventually lead to a higher capacity at mildly alkaline pH.

For graphene-based adsorbents, the ionic strength of the aqueous medium can also affect the adsorption mechanism of U. In general, ionic strength is the concentration of ions formed upon the dissociation of an ionic salt in water (Abelian et al., 2021). If the complexation of U species with the adsorbent surface is affected by the changes in the ionic strength of the solution, then adsorption is expected to occur by an outer sphere mechanism (Payne et al., 2013). This is because outer sphere mechanism reactions involve transfer of electrons between the two species without the inclusion of a covalent bond. Adsorption processes governed by the outer sphere mechanism do not involve bond formation, as they can be driven by non-covalent forces such as hydrophobic and electrostatic interactions (e.g., between U species and adsorbents surface) (Qiu et al., 2019). Conversely, an inner sphere mechanism is observed if ionic strength has little or moderate impact on U adsorption capacity (Dai et al., 2019a). This is because the inner sphere mechanism is promoted by covalent interactions between adsorbate ions and adsorbent active sites through metal complexation and/or coordination processes (Strawn, 2021). Likewise, in the case of an inner sphere mechanism, surface characteristics of the adsorbent can change significantly due to redox reactions with adsorbate molecules. Also, adsorption processes involving the outer sphere mechanism are faster since they have lower energy requirements than the inner sphere processes.

Most of the uranium removal studies conducted using graphene-based adsorbents follow the inner sphere mechanism due to covalent interactions between U species and functional groups present on the adsorbent surface. As an example, the adsorption capacity of U by graphene oxide sponge (GOS) remains unchanged in solutions with various ionic strengths in the range of 0 to 0.5 mol/L, suggesting U adsorption by the inner sphere mechanism (Liu et al., 2017). This is because of the affinity of surface functional groups (i.e., –COOH, –OH, and $–NH_2$) for U species, which eventually results in the formation of covalent linkages. Similar results were also observed for U removal by GO-Ch (Cheng et al., 2014) and mGO-PP adsorbents (Dai et al., 2019a). Hence, it can be concluded that the proportion and nature of U species in solution are pH dependent. Nonetheless, their interactions with graphene-based adsorbents depends on ionic strength due to the amphoteric nature of the functional groups present on the adsorbent surface (mainly oxygen and nitrogen containing functional groups).

7. Impact of interfering ions

Adsorption of heavy metal ions from aqueous solutions is profoundly affected by the presence of interfering ions. These interferences may be cationic to reduce the uptake of target metal ions as they can create a competitive domain due to the similar nature of the surface charge. Also, interfering ions may be anionic in nature, restricting the uptake of desired metal ions by making complexes which are not suitable for adsorption by the adsorbent. The major interfering ions are identified as cationic alkali/alkaline (Na, K, and Mg), cationic transition metal ions (Cu, Fe, Zn, and Ca), and anionic interfering ions (CO_3^{2-}, Cl^-, SO_4^{2-}, and NO_3^-) as they are commonly present in groundwater. Negatively charged OH^- ions from water can act as interferences as they can produce negatively charged species by forming the complexes with UO_2^{2+} ions. These negative U species are difficult to remove by graphene-based absorption because of electrostatic repulsion. However, the possibility of complexation between UO_2^{2+} ions and OH^- ions cannot be ignored as U adsorption processes take place in the aqueous phase.

The interference of cationic and anionic ions in the U adsorption process was investigated using pure GO and ammonia modified GO (NH_3-GO) (Verma and Dutta, 2015). Accordingly, Ca^{2+} ions tend to interfere with these adsorbents as they bear similar levels of positive charge as that of UO_2^{2+} ions (Fig. 5c). The adsorption capacity value of U is reduced by>50% in the presence of Ca^{2+} ions, reflecting the competing role of Ca^{2+} ions. In contrast, the adsorption capacity of U by NH_3-GO is found to be reduced by only ~ 30%. This may imply that the surface of NH_3-GO has a stronger affinity for U ions than the surface of GO adsorbents due to amine/amide functionalities. In the case of interfering anions, Cl^- shows the maximum interference with U adsorption, lowering the adsorption efficiency of NH_3-GO by 30%. This is because positively charged UO_2^{2+} ions can coordinate with Cl^- ions to form negatively charged $UO_2Cl_4^{2-}$, which cannot be adsorbed on NH_3-GO adsorbent. Similarly, the presence of SO_4^{2-} ions reduced the adsorption capacity of GO by 60% due to the formation of anionic $UO_2(SO_4)_2^{2-}$. The overall results demonstrated that NH_3-GO is more suitable for the selective uptake of U than GO. However, U adsorption capacity of NH_3-GO (40.1 mg/g) is lower than GO (72.2 mg/g) because of the lower zeta potential value in the working pH conditions. GO foam modified with phosphate groups (phos-GOF) did not undergo any apparent reduction in removal rates when Na^+ and K^+ were used as cationic impurities (Fig. 6) (Cai et al., 2019). However, the co-existence of divalent cations (e.g., Ca^{2+} and Mg^{2+}) suppresses the adsorption of U species on the adsorbent surface. Similarly, divalent anions ($CO_3^{2-}$and SO_4^{2-}) showed more significant effects on U removal than monovalent anions (Cl^-, and NO_3^-).

It is interesting to note that the use of HPO_4^{2-} as an interfering anion improves the effectiveness of the adsorption process. This is because sideways precipitation of U has been promoted in the form of solid $UO_2HPO_4{\cdot}4H_2O$. Phos-GOF adsorbent was found to have excellent reusability against U removal because of the presence of phosphate functional groups on its surface (Fig. 6). This is because phosphate group bearing active sites of phos-GOF adsorbent can easily be re-generated by acid treatment with a desorption efficiency of over 95%. Hence, it can be inferred that the presence of cationic and anionic interfering ions may cause a major reduction in U removal rates depending upon the nature of functional groups present on the surface of graphene. This may have an adverse effect on the performance of graphene-based adsorbents in real world applications as these ions are generally present in actual wastewater systems.

8. Performance evaluation of graphene-based adsorbents

Hummer's method is the most widely accepted technique for the preparation of GO by the oxidation of graphite in strong acids (Marcano et al., 2010). However, the extent of oxidation of graphene sheets largely depends on experimental conditions, and this influences the adsorption capacity values of GO. Also, as discussed above, the adsorption capacity of U is significantly affected by the solution pH, co-existing ions, and ionic strength of the test solution. Therefore, the impact of these parameters on U adsorption should be assessed precisely to apply graphene-based adsorbents for real-world situations.

In this section, we will evaluate the performances of various graphene-based adsorbents against U removal in terms of partition coefficient ($mg{\cdot}g^{-1}{\cdot}\mu M^{-1}$). Partition coefficient (PC) is a useful metric to describe the distribution pattern of a chemical compound between two phases at equilibrium conditions. In the case of adsorption, PC represents the ratio of target pollutant compounds in/on the surface of adsorbent to its amount in a liquid medium at equilibrium conditions. The significance of PC is to ensure and maintain the distribution of a chemical compound in adequate proportion within the employed experimental conditions. Here, partition coefficient values for U adsorption by graphene-based adsorbents were derived by normalizing adsorption capacity with residual U concentration in the liquid phase, as given below.

$$Partition\,coefficient(PC) = \frac{adsorption\,capacity\,of\,U\,species\,on\,adsorbent(mg/g)}{resiual\,U\,concentration(\mu M)}$$

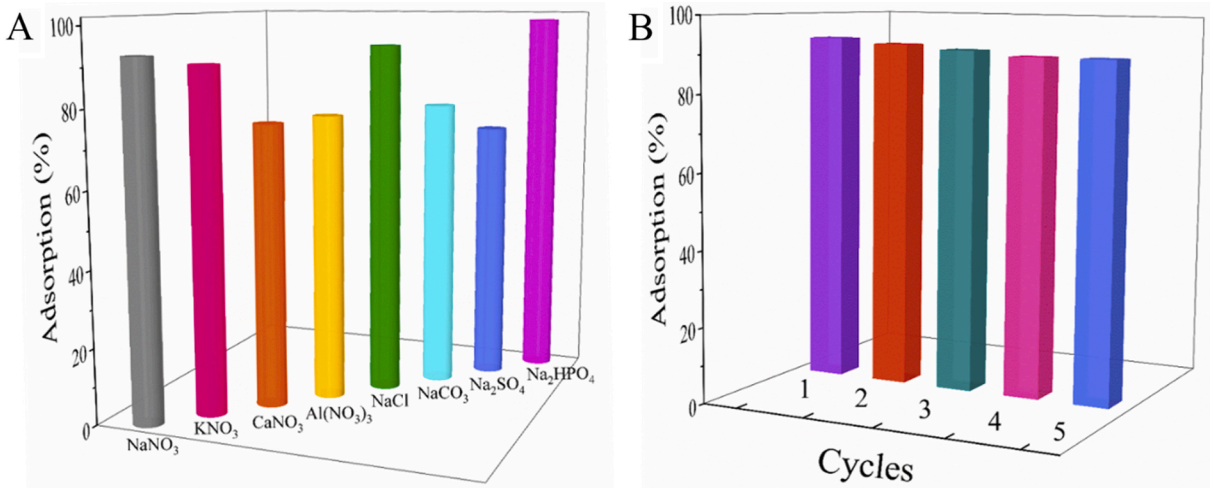

Fig. 6. The utility of phos-GOF adsorbents for removal of U: (A) Performance in relation to co-existing anions and cations and (B) reusability test (Cai et al., 2019).

8.1. GO adsorbents

The main driving force for U adsorption by graphene-based adsorbents is surface functional groups that can interact with U species. The number of oxygen functional groups introduced on graphene sheets and their resulting adsorption capacity depends heavily on the synthesis conditions. As such, various adsorption capacity values of U were observed for pure GO adsorbents in different studies as summarized in Table 1. As can be seen, few-layered GO prepared by the chemical oxidation of graphite flakes using a modified Hummer's method recorded the highest PC value of 23.67 $mg{\cdot}g^{-1}{\cdot}\mu M^{-1}$ corresponding to an adsorption capacity of 97.5 mg/g (Zhao et al., 2012). The few layered GO gives the highest PC value among all those reported in Table 1, although its adsorption capacity is not the highest. As such, PC can be used as a simple means to assess the possible bias in assessing the performance simply based on adsorption capacity. The observed superiority of few-layered GO may reflect the large surface area and high concentration of oxygen containing functional groups as it has a low C:O ratio (2.37). Large PC values signify the effectiveness of few-layered GO in removing almost 99% U at pH 5.0 from a solution (initial U concentration of 98.06 mg/L). In contrast, graphene oxides (GOs) prepared by the chemical oxidation of expanded graphite using a modified Hummer's method showed a very high Langmuir adsorption capacity of 138.89 mg/g at pH 4 as compared to that of few-layered GO. However, it recorded much lower partition coefficient value of 3.31 $mg{\cdot}g^{-1}{\cdot}\mu M^{-1}$ at an initial U concentration of 100 mg/L (Sun et al., 2015b). This reflects the fact that the concentration of unabsorbed U species is large in the case of GOs and can cause reduced performance as compared to few-layered GO. Such a high adsorption capacity of GOs is attributed to the high oxygen content of 37.43 wt% and surface area of 140.8 m^2/g.

Under similar experimental conditions, HOOC-GOs and rGOs showed lower adsorption capacities of 103.09 and 74.07 mg/g, respectively. This is because HOOC-GOs and rGOs contain fewer oxygen containing functional groups, which accounts for their lower capacities as compared to GOs. U adsorption capacities of GO adsorbents prepared by the chemical oxidation (CGO), electrolysis (EGO), and ball milling (BGO) techniques were also assessed at pH 4.5 (Wang et al., 2016c). It was found that the Langmuir adsorption capacity of CGO was 257. 23 mg/g, which is nearly three times higher than that of BGO (71.93 mg/g) and EGO (86.13 mg/g). This is because CGO contains higher amounts of oxygen containing functional groups than EGO and BGO. This result also indicates that the chemical oxidation of graphene sheets is the most suitable technique for the preparation of highly oxidized GO sheets for water remediation applications. The feasibility of commercially available industrial-grade multi-layer GO was also assessed for the removal of U at pH 6 (Wang et al., 2020a). Multi-layer GO adsorbent exhibited 66.51% removal of U with an adsorption capacity of 63.22 mg/g (and PC value of 4.49 $mg{\cdot}g^{-1}{\cdot}\mu M^{-1}$) at 10 mg/L of initial uranium content. The reason for the low percentage removal efficiency of the material is likely the very low oxygen content (>0.5%) in the sample, which inhibits the binding of U species with negatively charged active sites on the surface of GO.

8.2. Modified GO adsorbents

It is also feasible to enhance U adsorption capacity of GO by chemically modifying its surface bound oxygen containing functional groups as presented in Table 2. Several studies have reported the enhanced potential of nitrogen containing functional groups (like amine, amide, imine, and oximes) due to their high affinity for U species. Among various nitrogen functionalized GO adsorbents, the highest PC value of 513.40 $mg{\cdot}g^{-1}{\cdot}\mu M^{-1}$ was observed for graphene oxide–polyethyleneimine (GO-PEI) macrostructures against an initial U concentration of 100 mg/L (Huang et al., 2018). This corresponds to an adsorption capacity value of 215.6 mg/g at pH 5. High U chelation ability of GO-PEI adsorbent is attributed to the coordination of uranium ions with the amino and oxygen containing functional groups present on its surface. In contrast, the same adsorbent exhibited a significantly reduced adsorption capacity value of 30.5 mg/g at pH 3.5 due to the repulsive interactions between cationic UO_2^{2+} ions and protonated binding sites of the adsorbent. Another study also revealed that oxime-functionalized adsorbent (i.e., RGO-PDA/oxime) prepared by reducing GO sheets with a mixture of dopamine and salicylaldoxime in a tri-buffer solution at pH 8.5 is effective for U removal (Qian et al., 2018). The efficacy of RGO-PDA/oxime adsorbent for U adsorption was tested at various initial U levels (range

Table 1
A list of pure graphene oxide adsorbents for uranium removal from aqueous media.

Order	Adsorbent	Initial concentration (mg/L)	Temp. (K)	Time (h)	pH	Residual U conc. (μM)	Removal (%)	Adsorption capacity (mg/g)	Partition coefficient ($mg\ g^{-1}\ \mu M^{-1}$)	Ref.
1.	GO	142.8	R.T.	4	4	NA	22	299	0.64	(Li et al., 2012)
2.	GO	98.06	293	24	5	4.12	99	97.5	23.67	(Zhao et al., 2012)
3.	GO	32	303	24	4	105	22	138.2	1.32	(Liu et al., 2015b)
4.	GOs	100	293	48	4	42	90	138.89	3.31	(Sun et al., 2015a)
5.	GO	NA	298	48	3.45	NA	100	8.92	NC	(Wang et al., 2015a)
6.	GOs	2.38	293	48	5.2	0.50	95	11.3	22.67	(Wang et al., 2015b)
7.	GO	10	293	24	4.5	0.42	99	8.26	19.68	(Hu et al., 2016)
8.	CGO	59.5	298	2.5	4.5	49.98	80	257.23	5.15	(Wang et al., 2016c)
9.	GO	30	293	3	3.5	NA	NA	60.6	NC	(Lingamdinne et al., 2017)
10.	GO	85	298.15	3	6.5	NA	NA	97.3	NC	(Liu et al., 2018b)
11.	GO	10	293	24	4	0.55	98.7	9.34	3.37	(Mohamud et al., 2018)
12.	GO	100	298	6	5	241.5	42.5	575	2.38	(Qian et al., 2018)
13.	GO	10	298	0.5	4	6.30	85	16.03	2.54	(Yang et al., 2018)
14.	GOF	10	298	20	4	12.60	70	70	5.56	(Cai et al., 2019)
15.	GO	210	298	6	5	NA	NA	299.7	NC	(Li et al., 2019)
16.	GO	10	298	1	6	14.07	66.51	63.22	4.49	(Wang et al., 2020a)
17.	GONRs	60	298	4	4.5	126	50	153.5	1.22	(Li et al., 2021b)

Table 2
A list of modified graphene oxide adsorbents for uranium removal from aqueous media.

Order	Adsorbent	Initial concentration (mg/L)	Temp. (K)	Time (h)	pH	Residual U conc. (μM)	Removal (%)	Adsorption capacity (mg/g)	Partition coefficient (mg g^{-1} μM^{-1})	Ref.
1.	Polyaniline@GO	100	298	48	3	NA	NA	245.14	NC	(Sun et al., 2013)
2.	GO/ polypyrrole	27	298	48	5	2.27	98	147.1	64.86	(Hu et al., 2014)
3.	CD/ GO	24	288	24	5	20.16	80	103.9	5.15	(Song et al., 2014)
4.	GO/phytic acid	80	298	4	5.5	NA	NA	124.3	NC	(Liu et al., 2015a)
5.	PGO	32	303	24	4	90	33	251.7	2.80	(Liu et al., 2015b)
6.	3-D LDH/G	130	298	3	4	5.46	99	277.8	50.88	(Tan et al., 2015c)
7.	NH_3-GO	50	298	4	6	33.60	84	80.13	2.38	(Verma and Dutta, 2015)
8.	AOGONRs	59.5	298	4	4.5	NA	NA	502.6	NC	(Wang et al., 2015c)
9.	Polydopamine/ GO	10	293	24	4	4.20	90	145.39	34.62	(Zhao et al., 2015)
10.	AMGO	42.84	328	12	5.9	NA	NA	141.2	NC	(Chen et al., 2016)
11.	GO-NH_2	60	298	6	5.5	25.20	90	215.2	8.54	(Liu et al., 2016b)
12.	AGH	100	298	7	6	42.00	90	190.09	4.53	(Wang et al., 2016a)
13.	GOS	110	298.15	3	6	NA	NA	309.09	NC	(Zhang et al., 2016)
14.	rGO	30	293	3	3.5	NA	NA	84.5	NC	(Lingamdinne et al., 2017)
15.	EDTA-GO	60	298	6	6	29.48	88.3	212.77	7.22	(Liu et al., 2017)
16.	HO-CB[6]/GO	40	298	24	5	16.80	90	301.6	17.95	(Shao et al., 2017)
17.	SGO	10	293	48	2	0.00	100	45.05	NC	(Sun et al., 2017)
18.	CARGO-1	100	298	2	5	46.20	89	176	3.81	(Verma and Dutta, 2017)
19.	PEI-GHS	110	298	6	6	46.20	90	989	21.41	(Wang et al., 2017)
20.	GO-PEI	100	298	3	5	0.42	100	215.63	513.40	(Huang et al., 2018)
21.	GO-DTPAA	85	298.15	3	6.5	NA	NA	485	NC	(Liu et al., 2018b)
22.	COOH-GO	10	293	24	4	4.66	88.9	169.2	36.29	(Mohamud et al., 2018)
23.	RGO-PDA/oxime	100	298	6	5	NA	NA	1049	NC	(Qian et al., 2018)
24.	RGO-PDA	100	298	6	5	NA	NA	650	NC	(Qian et al., 2018)
25.	Phos-GOF	10	298	24	4	2.73	93.5	93.5	34.25	(Cai et al., 2019)
26.	GO/PDA/PAO	10	298	6	6	NA	100	240.9	NC	(Dai et al., 2019b)
27.	MBTA-GO	250	298	2	3.5	NA	NA	264	NC	(Ding et al., 2019)
28.	RGO-AMP	10	298	0.5	6	2.77	93.4	186.80	67.39	(Dutta et al., 2019)
29.	GOANS	250	298	1	4	105.00	90	311.5	2.97	(Gado et al., 2019)
30.	GO-pDA	210	298	6	5	NA	NA	314	NC	(Li et al., 2019)
31.	GO-pDA-PEI	210	298	6	5	37.04	95.8	416	11.23	(Li et al., 2019)
32.	HGP	100	NA	0.34	5	14.70	96.50	545.7	37.12	(Liao et al., 2019)
33.	GO-CMC	100	313	3	5	42.00	90	322.6	7.68	(Peng et al., 2019)
34.	GO/PEDOT:PSS	10	298	24	4.5	0.00	100	48.90	NC	(Song et al., 2019)
35.	MGO	20	NA	1	6	0.66	99.21	86.15	129.82	(Wang et al., 2020a)
36.	GO-DM-AO	478.7	298	0.5	8	201.05	90	935	4.65	(Yang et al., 2019b)
37.	GA/GNRs	250	298	4	5	NA	NA	327.8	NC	(Hu et al., 2020)
38.	GA	42	298	24	4	NA	NA	238.67	NC	(Zhao et al., 2019)
39.	GO-HDX	250	298	1.33	4	14.91	98.58	58.5	3.92	(Atia et al., 2020)
40.	PAO-GH	300	298	4	4	NA	NA	222.2	NC	(Bai et al., 2020)
41.	P-pFGO-7	134	298	1	4	73.16	87	266.7	3.65	(Lei et al., 2020)
42.	PAO/GONRs	59.5	298	4	4.5	67.47	73	216	3.2	

(*continued on next page*)

Table 2 (*continued*)

Order	Adsorbent	Initial concentration (mg/L)	Temp. (K)	Time (h)	pH	Residual U conc. (μM)	Removal (%)	Adsorption capacity (mg/g)	Partition coefficient (mg g^{-1} μM^{-1})	Ref.
										(Wang et al., 2021a)
43.	GO/HAP	40	298	2	3	11.76	93	373	31.72	(Su et al., 2021)
44.	GO-pAM-MBA	301	298	5	4	37.93	97	589.1	15.53	(Yang et al., 2021b)

8–100 mg/L). Similar masses of control adsorbents, i.e., GO and GO reduced with dopamine (RGO-PDA), were also tested for U to recognize the contribution of oxime molecules in the U removal (Qian et al., 2018). Accordingly, all three adsorbents (RGO-PDA/oxime, RGO-PDA, and GO) follow the Langmuir adsorption isotherm model with high adsorption capacity values of 1049, 675, and 613 mg/g, respectively. The excellent performance of RGO-PDA/oxime towards U adsorption is ascribed to the high affinity of deprotonated C = N-OH moieties of oxime molecules for uranium ions (Gunathilake et al., 2015). This also implies that oxime molecules are present at the outer surface of RGO-PDA/oxime adsorbent to facilitate U adsorption. On the other hand, PDA molecules act as a bridge to connect oxime molecules with the GO surface as shown in Fig. 7. This type of molecular bridging stabilizes the RGO-PDA/oxime by minimizing the electrostatic repulsive forces. Other factors which enable U uptake by RGO-PDA/oxime adsorbent are its porous 3D network and large surface area.

Phosphate and sulfur functionalized graphene adsorbents were also prepared for the treatment of U from aqueous solutions (Liu et al., 2015b; Zhang et al., 2016; Sun et al., 2017; Cai et al., 2019). As an example, fully phosphorylated 3D graphene oxide foam (phos-GOF) was prepared by the hydrothermal treatment of GO with phytic acid, as shown in Fig. 8 (Cai et al., 2019). The adsorption capacities and PC value of phos-GOF were 93.5 mg/g and 34.25 $mg{\cdot}g^{-1}{\cdot}\mu M^{-1}$ at an initial U concentration of 10 mg/L. The existence of phosphorus containing functional groups on a phos-GOF surface appears to endow it with excellent affinity for U species. Moreover, spend phos-GOF adsorbent can be easily regenerated with 0.02 mol/L HNO_3 to maintain the high adsorption efficiency (e.g., ~93.5% up to five test cycles). In contrast, non-phosphorylated GOF adsorbent exhibited a much smaller adsorption capacity of nearly 70 mg/g with a PC value of 5.56 $mg{\cdot}g^{-1}{\cdot}\mu M^{-1}$ against an initial U concentration of 10 mg/L. The high affinity and contribution of phosphate functionalities towards U removal was also observed in phosphate functionalize GO (PGO) prepared by grafting triethyl phosphite groups onto a GO surface (Liu et al., 2015b). It was observed that the electrostatic interactions prevailing between U species and phosphate/oxygen functional groups of GO were responsible for the selective U uptake from acidic solution. On a similar note, GO was chemically functionalized to incorporate sulfonyl groups (–OSO_3H) on its surface (Zhang et al., 2016; Sun et al., 2017). GOS adsorbent prepared by treating GO with fuming sulphonic acid (i.e., SO_3 in H_2SO_4) showed a high U adsorption capacity of 309.1 mg/g at pH 6 with an initial U concentration of 110 mg/L (PC = ?) (Zhang et al., 2016). On the other hand, sulfonated GO (SGO) prepared by the treatment of pre-oxidized graphite with H_2SO_4 and $KMnO_4$ exhibited a smaller maximum adsorption capacity of 45.1 mg/g at ultralow pH of 2 (PC = ?) (Sun et al., 2017). Almost complete removal of U by SGO adsorbent suggests its enhanced performance at low pH conditions.

GO adsorbents with multiple functionalities or chelating sites were also developed for the efficient removal of U species. In this context, novel functionalized graphene adsorbents have been developed by treating GO with adenosine-5'-monophospahte (RGO-AMP) and poly amino-phosphonic acid (PAMGO) (Dutta et al., 2019; Yin et al., 2019). These functional groups (e.g., amide/amide and phosphates) grafted on GO surface can induce strong interactions between adsorbents and U species. The partition coefficient value for RGO-AMP adsorbent was 67.39 $mg{\cdot}g^{-1}{\cdot}\mu M^{-1}$, corresponding to an adsorption capacity value of 186.8 mg/g for a uranium aqueous solution (10 mg/L concentration). This RGO-AMP adsorbent follows the Langmuir isotherm model, which suggests the importance of monolayer accumulation of U species on the

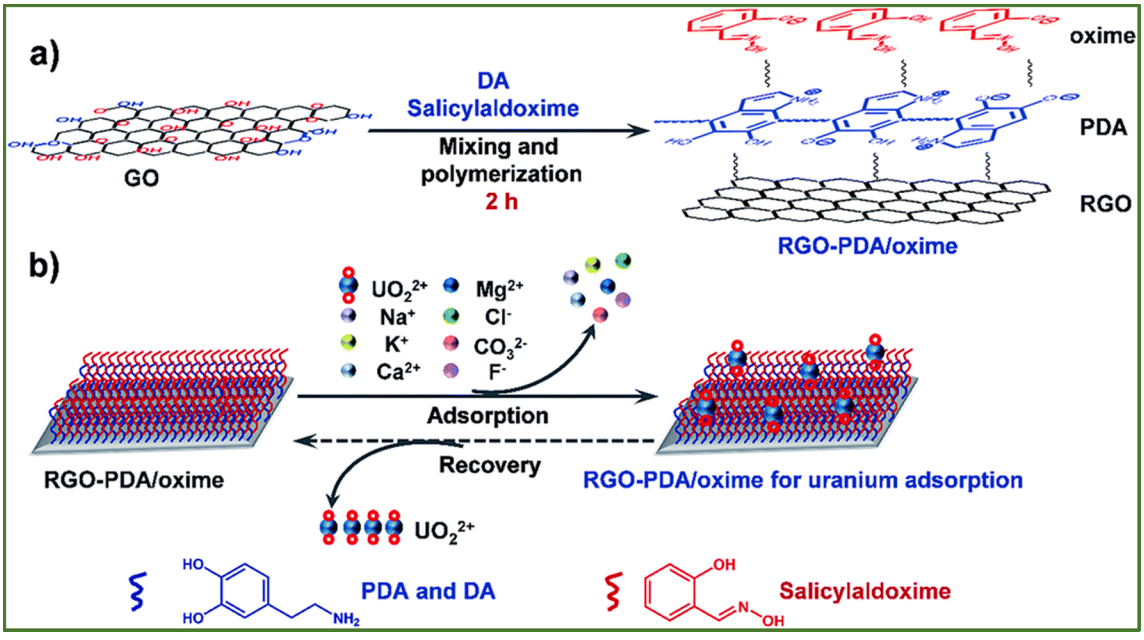

Fig. 7. Application of RGO-PDA/oxime toward U removal: (a)Schematic of the synthesis of the RGO-PDA/oxime and (b) the adsorption of uranium by the prepared RGO-PDA/oxime (Qian et al., 2018).

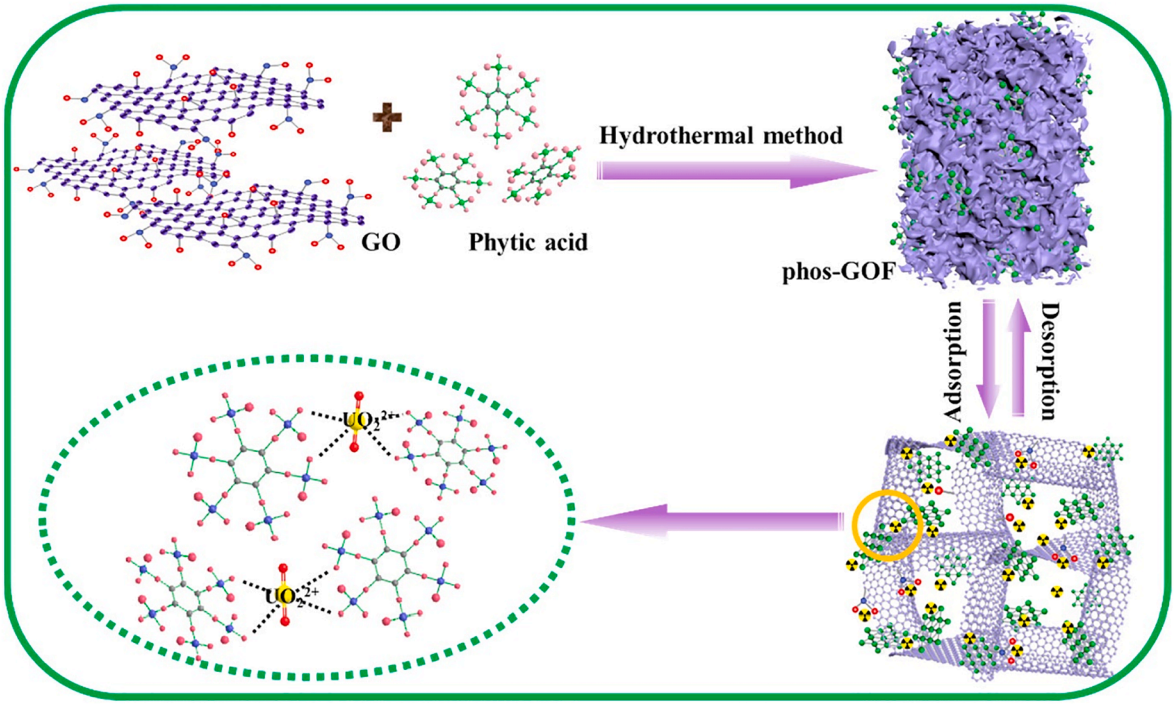

Fig. 8. Schematic of the preparation of phos-GOF and the main adsorption mechanism of U(VI) on phos-GOF (Cai et al., 2019).

adsorbent surface. In addition, the small equilibration time of 240 s for a U uptake of up to ~ 93% indicates high chelation tendency and affinity of amide/amide and phosphates functional groups for U. The utility of amino-phosphorous moieties in uranium removal is also evident in other adsorbent materials (Zhang et al., 2020). Thus, chemical modification of GO to add nitrogen, phosphorus, and sulfur moieties in graphene skeleton can serve as major binding sites to lead to the removal of uranium from wastewaters.

8.3. Graphene-metal oxide composite adsorbents

GO exhibits extreme hydrophilicity in aqueous solutions because of the presence of a large amount of oxygen containing polar functionalities on its surface. This discourages the use of pure GO in wastewater treatment and adsorption processes due to associated post-separation complexities. As an effective solution for such a limitation is to impregnate or load magnetic nanomaterials on GO sheets to provide easy and quick separation with the aid of an external magnetic field (Zong et al., 2013). Also, collaborative association of the adsorption efficiencies of GO and magnetic nanomaterials is favorable for obtaining high adsorption capacity. A list of such graphene-metal oxide composites developed for the removal of aqueous phase U is presented in Table 3. The adsorption performances of graphene-metal oxide composites are far superior to the pure GO adsorbents (Table 1). Magnetic GO based adsorbents, i.e., polyamidoxime/polyethyleneimine magnetic graphene oxide (mGO-PP), was developed by the in-situ polymerization of acrylonitrile on polyethyleneimine bonded magnetic GO (Dai et al., 2019a). Results of>90% removal of U (within first 30 min) from simulated wastewater with 10 mg/L U at pH 6 indicates rapid uptake of U. The adsorption capacity of mGO-PP was determined as 200.4 mg/g, and the corresponding PC was estimated as 4747.6 $mg{\cdot}g^{-1}{\cdot}\mu M^{-1}$. A large PC value implies high potency of mGO-PP adsorbent towards U removal, which is attributed to the high affinity of the nitrogen containing functional groups grafted on the surface of magnetic GO. The suitability of mGO-PP adsorbent for real applications was also investigated by treating actual mine radioactive wastewater with U ions concentration of 100.8 μg/L along with common metal ions. The mGO-PP showed selective adsorption of U from actual mine wastewater with a high removal rate of 93.68%. The PC value for the treatment of mine wastewater was 70.83 $mg{\cdot}g^{-1}{\cdot}\mu M^{-1}$. The residual concentration of U in the mine wastewater was 6.37 μg/L, which is significantly lower than the permissible limits of uranium (30 μg/L) established by WHO (Verma and Dutta, 2015). Thus, it can be inferred that GO adsorbents bearing nitrogen moieties are beneficial for the selective uptake of U species from artificial as well as real waste waters.

The adsorption capacity of GO sheets was also enhanced by loading manganese oxide nanoparticles because of the synergistic effects between active binding sites of both (Yang et al., 2018). Accordingly, almost 99% of U was removed from 10 mg/L of U solution when 0.5 g/L mass of graphene oxide-manganese oxide (GOMO) adsorbent was used at pH 4. In contrast, a similar extent of U removal occurred at much higher does (e.g., 1.0 g/L) of pure GO under the same experimental conditions. The adsorption capacity values for GO and GOMO adsorbent when measured at pH 4 were 16.03 and 19.92 mg/g, respectively, with their corresponding PC values of 2.54 and 474.29 $mg{\cdot}g^{-1}{\cdot}\mu M^{-1}$, respectively. The higher adsorption capacity of GOMO might reflect the contribution of active sites from MnO_2 nanoparticles as they also contributed to the increases in the total number of active sites on GOMO adsorbents (e.g., relative to GO). It is important to note that there are drastic differences in the performance between mGO-PP (adsorption capacity = 200.4 mg/g; PC = 4771.43 $mg{\cdot}g^{-1}{\cdot}\mu M^{-1}$) and GOMO adsorbents (adsorption capacity = 19.92 mg/g; PC = 474.29 $mg{\cdot}g^{-1}{\cdot}\mu M^{-1}$). This large difference between the two adsorbents demonstrates the extraordinary contribution of nitrogen containing functional groups of mGO-pp in removing U from an aqueous solution. In addition, GO composites with metal oxide such as TiO_2 (Yu et al., 2019), Fe:Ni (Zhang et al., 2019b), $NiCo_2O_4$ (Song et al., 2016), and $CoFe_2O_4$ (Tan et al., 2015a) also showed high adsorption capacity values of 441.3, 384.6, 349, and 125 mg/g, respectively, with the corresponding PC values of 13.13, 4.53, 9.23, and 59.52 $mg{\cdot}g^{-1}{\cdot}\mu M^{-1}$. Hence, it can be concluded that the adsorption capacity of GO sheets can be improved considerably through the incorporation of metal oxides.

Table 3
A list of graphene-metal oxide composite adsorbents for uranium removal from aqueous media.

Order	Adsorbent	Initial concentration (mg/L)	Temp. (K)	Time (h)	pH	Residual U conc. (μM)	Removal (%)	Adsorption capacity (mg/g)	Partition coefficient (mg g^{-1} μM^{-1})	Ref.
1.	AOMGO	47.6	298	24	5	2.00	99	76.87	38.45	(Zhao et al., 2013)
2.	Fe_3O_4/GO	26.65	293	24	5.5	50.37	55	69.49	1.38	(Zong et al., 2013)
3.	GO/SiO_2	5	298.15	0.12	4	0.21	99	17.89	85.19	(Meng et al., 2015)
4.	$CoFe_2O_4$-rGO	50	298	4	6	2.10	99	125	59.52	(Tan et al., 2015a)
5.	MnO_2-Fe_3O_4-rGO	120	328	6.667	6	37.40	92.58	108.7	2.91	(Tan et al., 2015b)
6.	α-GOM_2	40	298	0.5	3.8	NA	–	185.2	NC	(Pan et al., 2016)
7.	Cucurbit[6]uril/ GO-Fe_3O_4	36	298	24	5	30.24	80	122.48	4.05	(Shao et al., 2016)
8.	$NiCo_2O_4$@rGO	150	298	9	5	37.80	94	349	9.23	(Song et al., 2016)
9.	rGONF	30	293	3	3.5	NA	–	200	NC	(Lingamdinne et al., 2017)
10.	GONF	30	293	3	3.5	NA	–	135.13	NC	(Lingamdinne et al., 2017)
11.	FG-20	100	298	2	6	39.90	90.5	455	11.40	(El-Maghrabi et al., 2017)
12.	mGO-PAO	10	313	24	6	0.74	98.24	24.89	33.67	(Dai et al., 2018)
13.	GOMO	10	298	0.5	4	0.04	99.99	19.92	474.29	(Yang et al., 2018)
14.	SMGO	10	298	3	4	4.20	90	28.2	6.71	(Choi et al., 2019)
15.	mGO-PP	10	298	24	6	0.04	99.99	200.4	4747.62	(Dai et al., 2019a)
16.	AO/mGO	10	293	48	4	0.84	98	10.438	12.43	(Hu et al., 2019)
17.	MGs	10	298	2	5	8.40	80	271.7	32.35	(Ma et al., 2019)
18.	rGO/Fe_3O_4/TW	10	298	2	5	0.42	99	19.8	47.14	(Yang et al., 2019a)
19.	3D GA/TiO_2	20	298	12	5	33.60	60	441.3	13.13	(Yu et al., 2019)
20.	GO/Al_2O_3	20	293	0.5	6.5	21.00	75.00	142.8	6.80	(Zhang et al., 2019a)
21.	Fe:Ni/GO	59.5	298	6	5.5	84.97	66	384.62	4.53	(Zhang et al., 2019b)
22.	FFGS	60	303	NA	5	NA	–	219.71	NC	(Zhu et al., 2019b)
23.	FH/GO	60	303	NA	5	NA	–	196.24	NC	(Zhu et al., 2019b)
24.	FH/Fe_3O_4	60	303	NA	5	NA	–	181.98	NC	(Zhu et al., 2019b)
25.	FH	60	303	NA	5	NA	–	100.83	NC	(Zhu et al., 2019b)
26.	CMC/MGOs	72.11	301	NA	5.5	131.08	56.72	188.97	1.44	(Zong et al., 2019)
27.	GO/FeS	140	298	2	5	6.23	98.94	251	40.27	(Li et al., 2021a)
28.	GO/Fe_2O_3/GC	10		0.5	5	0.55	98.7	66.36	121.54	(Yang et al., 2021a)

8.4. Miscellaneous graphene adsorbents

GO composites with many other materials such as activated carbon, activated sludge, metal organic frameworks (MOFs), polysaccharides (e.g., chitosan, sodium alginate, and agar), clay minerals (e.g., bentonite, montmorillonite, and sepiolite), and biomaterial (e.g., bovine serum albumin) have been developed to achieve efficient removal of U from aqueous media, as summarized in Table 4. In particular, MOFs are widely employed to prepare adsorbents for water remediation applications because of their advantageous porous network structure. Among various GO-MOF composites adsorbents, rGO-ZIF67 aerogel showed an excellent adsorption capacity value of 1889 mg/g at an initial U concentration of 300 mg/L with a PC value of 1498.85 $mg{\cdot}g^{-1}{\cdot}\mu M^{-1}$ and a high removal rate of almost 99.9% (Zhao et al., 2020). The extraordinary performance of rGO-ZIF67 aerogel is attributed to the large specific surface area and porous network with residual oxygen moieties. In short, U uptake by rGO-ZIF67 aerogel is facilitated by surface complexation and an electrostatic attraction mechanism. In contrast, MIL-68/GO composites prepared using solvothermal process revealed the lowest PC value of 2.23 $mg{\cdot}g^{-1}{\cdot}\mu M^{-1}$(Zhu et al., 2019a). The composite nonetheless revealed moderately high adsorption capacity value of 375 mg/g as tested on simulated wastewater at high initial U concentration of 400 mg/L. The high adsorption capacity of MIL-68/GO composites is ascribable to its porous network structure to facilitate the interaction of U with active sites with –OH and –COOH functionalities. Thus, it can be concluded that graphene-MOF composite adsorbents are highly recommended for the treatment of U in aqueous solutions.

GO composites were also developed with chitosan to enable U removal by the active functional moieties present in chitosan in addition to those present on the surface of GO. Chitosan is a natural polysaccharide material composed of randomly distributed N-acetyl glucosamine and D-glucosamine units attached via β-linkages (Verma and Dutta, 2020). The presence of large numbers of amino ($–NH_2$) and hydroxyl (–OH) groups on chitosan can promote effective removal of heavy metal ions. However, the low mechanical/chemical stability of chitosan restricts its usage in commercial applications. On the other

Table 4
List of miscellaneous graphene adsorbents for uranium removal from aqueous media.

Serial no.	Adsorbent	Initial concentration (mg/L)	Temp. (K)	Time (h)	pH	Residual U conc. (μM)	Removal (%)	Adsorption capacity (mg/g)	Partition coefficient (mg g^{-1} μM^{-1})	Ref.
1.	GO-ACF	50	298	1	5.5	NA	–	298	NC	(Chen et al., 2013)
2.	GO@sepiolite	50	298	24	5	NA	–	161.29	NC	(Cheng et al., 2013)
3.	GO-Ch	40.46	303	24	4	42.48	75	225.78	5.31	(Cheng et al., 2014)
4.	Agar-MMT-GO	15	303	24	4.5	11.34	82	142.8	12.59	(Cheng et al., 2017)
5.	GO-CS	300	R.T.	6	8.3	1.26	99.9	384.6	305.24	(Huang et al., 2017)
6.	GO–BSA composites	200	298	1.33	6	16.80	98	389	23.15	(Yang et al., 2017)
7.	Cal-Alg-GO	1000	298	24	5	NA	–	29.4	NC	(Basu et al., 2018)
8.	GO15-MIL-101 (Fe)	10	298	24	5.5	10.50	75	106.89	10.18	(Han et al., 2018)
9.	GO@PDA/CS	50	298	0.25	6	7.35	96.5	161	21.90	(Liao et al., 2018)
10.	GO/bentonite	15	303	3	7	6.30	90	33.68	5.35	(Liu et al., 2018a)
11.	o-GS-COF	300	298	2	4.5	NA	–	220.1	NC	(Wen et al., 2018)
12.	SPG	1000	298	4	4	NA	–	403.78	NC	(Yi et al., 2018)
13.	AS-GO	25	308	2	4	NA	–	180.6	NC	(Zhao et al., 2018)
14.	GZA	200	298	12	7	168.00	80	316.48	1.88	(Guo et al., 2019)
15.	GO-BSA	100	313	3	5	42.00	90	270	6.43	(Peng et al., 2019)
16.	MIL-68/GO	400	298	3	8	168.00	90	375	2.23	(Zhu et al., 2019a)
17.	GO-CMC-AO	200	308	3	6	84.00	90	306.98	3.65	(Yang et al., 2020)
18.	GO-CS-AO	200	308	3	6	84.00	90	243.36	2.90	(Yang et al., 2020)
19.	GCZ8A	150	298	3	8	NA	–	361.01	NC	(Guo et al., 2020)
20.	rGO/ZIF 67	300	298	48	4.01	1.26	99.9	1888.55	1498.85	(Zhao et al., 2020)

hand, graphene exhibits a high tensile strength with a high Young's modulus of 1 TPa (Kumar and Srivastava, 2018). The adsorbents developed by the association of GO with chitosan are environmentally friendly as they are free from any metallic component. A three dimensional graphene oxide-chitosan (GO-CS) aerogel was demonstrated for a high U adsorption capacity of 384.6 mg/g (PC = 305.24 $mg{\cdot}g^{-1}{\cdot}\mu M^{-1}$) at pH 8.3 (Huang et al., 2017). This enhanced performance of GO-CS supports the advantage of using aerogel-based adsorbents in metal removal applications. GO gels modified with amidoxime groups and polysaccharides (i.e., carboxy methyl cellulose and chitosan) are also observed to have high adsorption capacity values of 307.0 and 243.4 mg/g, respectively (Yang et al., 2020). The PC values for GO-CMC-AO and GO-CS-AO were 3.65 and 2.90 $mg{\cdot}g^{-1}{\cdot}\mu M^{-1}$, respectively. Likewise, aerogels of chitosan with polydopamine modified GO (GO@PDA/CS) showed a high U adsorption capacity of 161 mg/g and PC value of 21.9 $mg{\cdot}g^{-1}{\cdot}\mu M^{-1}$ (Liao et al., 2018). Hence, aerogels consisting of graphene and chitosan (or other polysaccharides like cellulose) exhibit high U adsorption efficiency due to its porous network and existence of active sites on its surface.

9. Summary and outlook

In this article, we discussed emerging applications of graphene-based adsorbents in the adsorptive removal of uranium ions from wastewater. Graphene has attracted widespread attention for the remediation of heavy and toxic metal ions, including radioactive elements like U due to its large surface area, electronic properties, and tunable surface characteristic and strength. We have discussed practical strategies to obtain high and rapid adsorption of U species in detail. Functionalization and composite formation are major approaches to enhance adsorption capacity of graphene adsorbents. U adsorption on graphene-based adsorbents widely depends upon the existing functional moieties. Diverse functional moieties containing hetero-atoms such as oxygen, nitrogen, phosphorus, and sulfur both promote facile

adsorption of U species and drive selective uptake of U from the aqueous solutions over other metal ions. These functionalities are helpful in controlling U adsorption based on electrostatic forces such as cation-π interactions and covalent forces like complexation and hard-hard interactions. Further, pH should also have major influence on U adsorption processes as the speciation of U varies across pH values. Moreover, pH significantly affects the surface charge of graphene-based adsorbents, controlling the U removal efficiency.

Graphene oxide is the most widely used derivative of graphene. GO is an extremely hydrophilic derivative of graphene due to the presence of a large amount of oxygen functionalities (e.g., hydroxyl and carbonyls). As such, it can trigger unnecessary difficulties in post-separation stages, requiring costly and high-capacity separating devices (e.g., centrifuge with high operating speed or syringe filters). In this context, if the GO surface is modified with fewer hydrophilic functional groups, it can help in stabilizing the GO sheets in solutions. This also enhances thermal stability of GO sheets to impart their uniform distribution for the rapid scanning of the available U species. The adsorption performance of most of the chemically modified GO adsorbents is far better than GO because of the active moieties of functionalities (for example amine, amide, oxime, phosphate, and sulfates). Likewise, coupling of graphene with nanomaterials is a useful option to improve the efficacy of the adsorption process as the active binding sites from both components can promote U removal. The use of GO composites with magnetic nanomaterials is also an effective option for the rapid separation of adsorbent using external magnets. However, it is of prime importance to develop effective separation protocol for the post-treatment of graphene-based adsorbents (including other carbon materials) from the tested solutions due to its biotoxicity in humans and animals (Pikula et al., 2018; Haixia et al., 2021). According to a recent study on biological behavior of graphene, it was fond out that graphene family materials can adhere to outer surface of cell membrane or interact with the lipid bilayers of the plasma membrane. They can also agglomerate into the plasma membrane to induce inflammatory conditions with the leakage of cytoplasmic fluid (Magne et al., 2021). Considering all the issues raised above, the following key points should be considered to expand the utility of graphene-based adsorbents for practical applications toward the removal of uranium and/or other toxic metal ion pollutants from aqueous media.

1. Future research in this area should be aimed at producing a graphene-based adsorbent with functional groups specific for uranium abstraction from solutions. This will help in employing graphene-based adsorbents for real applications as effluent from a radioactive plant contains many other metallic species at the same time.
2. Emphasis should be placed on designing an adsorbent material that could simultaneously remove different types of U species from solution. This would help overcome the pH barrier restrictions to help expand the application of graphene-based adsorbents.
3. Efficient protocols should be developed for the post treatment separation of graphene adsorbents in light of associated health hazards. Green and cost-effective synthesis methods for GO should also be used to avoid the consumption of toxic chemicals in adsorbent synthesis.
4. Adsorbents with short equilibration time and large capacities should be developed for quick U adsorption. Also, the surface properties of the adsorbent should not change drastically with pH to achieve consistency in U removal across varying pH values.
5. The major drawback of handling uranium polluted water is the radioactivity. Hence, spent adsorbent should be discarded with special caution at regulated sites so that it does not have any adverse effects on humans or ecological systems.

Declaration of Competing Interest

The authors declare that they have no known competing financial interests or personal relationships that could have appeared to influence the work reported in this paper.

Acknowledgement

This work was supported by a grant from the National Research Foundation of Korea (NRF) funded by the Ministry of Science and ITC (MSIT) of Korean government (Grant No: 2021R1A3B1068304).

References

Abdeen, Z., Akl, Z.F., 2015. Uranium(vi) adsorption from aqueous solutions using poly (vinyl alcohol)/carbon nanotube composites. RSC Adv. 5, 74220–74229.
Abelian, A., Dybek, M., Wallach, J., Gaye, B., Adejare, A., 2021. Chapter 6 - Pharmaceutical chemistry. in: Adejare, A. (Ed.). Remington (Twenty-third Edition). Academic Press, pp. 105–128.
Ahmad, M., Wang, J., Yang, Z., Zhang, Q., Zhang, B., 2020. Ultrasonic-assisted preparation of amidoxime functionalized silica framework via oil-water emulsion method for selective uranium adsorption. Chem. Eng. J. 389, 124441.
Alahabadi, A., Singh, P., Raizada, P., Anastopoulos, I., Sivamani, S., Dotto, G.L., Landarani, M., Ivanets, A., Kyzas, G.Z., Hosseini-Bandegharaei, A., 2020. Activated carbon from wood wastes for the removal of uranium and thorium ions through modification with mineral acid. Colloids Surf., A 607, 125516.
Allen, M.J., Tung, V.C., Kaner, R.B., 2010. Honeycomb Carbon: A Review of Graphene. Chem. Rev. 110, 132–145.
Amphlett, J.T.M., Choi, S., Parry, S.A., Moon, E.M., Sharrad, C.A., Ogden, M.D., 2020. Insights on uranium uptake mechanisms by ion exchange resins with chelating functionalities: Chelation vs. anion exchange. Chem. Eng. J. 392, 123712.
Asic, A., Kurtovic-Kozaric, A., Besic, L., Mehinovic, L., Hasic, A., Kozaric, M., Hukic, M., Marjanovic, D., 2017. Chemical toxicity and radioactivity of depleted uranium: The evidence from in vivo and in vitro studies. Environ. Res. 156, 665–673.
Atia, B.M., Gado, M.A., Abd El-Magied, M.O., Elshehy, E.A., 2020. Highly efficient extraction of uranyl ions from aqueous solutions using multi-chelators functionalized graphene oxide. Sep. Sci. Technol. 55, 2746–2757.
Ayawei, N., Ebelegi, A.N., Wankasi, D., 2017. Modelling and Interpretation of Adsorption Isotherms. J. Chem. 2017, 3039817.
Bai, J., Chu, J., Yin, X., Wang, J., Tian, W., Huang, Q., Jia, Z., Wu, X., Guo, H., Qin, Z., 2020. Synthesis of amidoximated polyacrylonitrile nanoparticle/graphene composite hydrogel for selective uranium sorption from saline lake brine. Chem. Eng. J. 391, 123553.
Baker, I., 2018. Uranium/Uranium Oxide. Fifty Materials That Make the World. Springer, pp. 251-254.
Banning, A., 2020. Geogenic arsenic and uranium in Germany: Large-scale distribution control in sediments and groundwater. Journal of Hazardous Materials, 124186.
Basu, H., Singhal, R.K., Pimple, M.V., Saha, S., 2018. Graphene oxide encapsulated in alginate beads for enhanced sorption of uranium from different aquatic environments. J. Environ. Chem. Eng. 6, 1625–1633.
Belgacem, A., Rebiai, R., Hadoun, H., Khemaissia, S., Belmedani, M., 2014. The removal of uranium (VI) from aqueous solutions onto activated carbon developed from grinded used tire. Environ. Sci. Pollut. Res. 21, 684–694.
Bigalke, M., Schwab, L., Rehmus, A., Tondo, P., Flisch, M., 2018. Uranium in agricultural soils and drinking water wells on the Swiss Plateau. Environ. Pollut. 233, 943–951.
Brugge, D., 2014. Uranium. In: Wexler, P. (Ed.), Encyclopedia of Toxicology, Third Edition. Academic Press, Oxford, pp. 883–884.
Cai, Y., Wang, X., Feng, J., Zhu, M., Alsaedi, A., Hayat, T., Tan, X., 2019. Fully phosphorylated 3D graphene oxide foam for the significantly enhanced U(VI) sequestration. Environ. Pollut. 249, 434–442.
Chabot, V., Higgins, D., Yu, A., Xiao, X., Chen, Z., Zhang, J., 2014. A review of graphene and graphene oxide sponge: material synthesis and applications to energy and the environment. Energy Environ. Sci. 7, 1564–1596.
Chen, L., Zhao, D., Chen, S., Wang, X., Chen, C., 2016. One-step fabrication of amino functionalized magnetic graphene oxide composite for uranium (VI) removal. J. Colloid Interface Sci. 472, 99–107.
Chen, S., Hong, J., Yang, H., Yang, J., 2013. Adsorption of uranium (VI) from aqueous solution using a novel graphene oxide-activated carbon felt composite. J. Environ. Radioact. 126, 253–258.
Cheng, H., Zeng, K., Yu, J., 2013. Adsorption of uranium from aqueous solution by graphene oxide nanosheets supported on sepiolite. J. Radioanal. Nucl. Chem. 298, 599–603.
Cheng, W., Ding, C., Nie, X., Duan, T., Ding, R., 2017. Fabrication of 3D macroscopic graphene oxide composites supported by montmorillonite for efficient U (VI) wastewater purification. ACS Sustainable Chem. Eng. 5, 5503–5511.
Cheng, W., Wang, M., Yang, Z., Sun, Y., Ding, C., 2014. The efficient enrichment of U (VI) by graphene oxide-supported chitosan. RSC Adv. 4, 61919–61926.
Choi, Y.-L., Choi, J.-S., Lingamdinne, L.P., Chang, Y.-Y., Koduru, J.R., Ha, J.-H., Yang, J.-K., 2019. Removal of U(VI) by sugar-based magnetic pseudo–graphene oxide and its application to authentic groundwater using electromagnetic system. Environ. Sci. Pollut. Res. 26, 22323–22337.

Chua, C.K., Pumera, M., 2014. Chemical reduction of graphene oxide: a synthetic chemistry viewpoint. Chem. Soc. Rev. 43, 291–312.
Courtois, J., Wang, B., Abonee, I.N., Kun, X., Tian, Q., Yan, M., Gibaud, A., 2020. Bare and polyelectrolyte-coated calcium carbonate particles for seawater uranium extraction: an eco-friendly alternative. Sustainable Energy Fuels 4, 5301–5312.
Dai, Z., Sun, Y., Zhang, H., Ding, D., Li, L., 2019a. Highly Efficient Removal of Uranium (VI) from Wastewater by Polyamidoxime/Polyethyleneimine Magnetic Graphene Oxide. J. Chem. Eng. Data 64, 5797–5805.
Dai, Z., Sun, Y., Zhang, H., Ding, D., Li, L., 2019b. Rational Synthesis of Polyamidoxime/Polydopamine-Decorated Graphene Oxide Composites for Efficient Uranium(VI) Removal from Mine Radioactive Wastewater. Ind. Eng. Chem. Res. 58, 19280–19291.
Dai, Z., Zhang, H., Sui, Y., Ding, D., Li, L., 2018. Preparation of Polyamidoxime/Magnetic Graphene Oxide Composite and Its Application for Efficient Extraction of Uranium (VI) from Aqueous Solutions in an Ultrasonic Field. J. Chem. Eng. Data 63, 4215–4225.
de Assis, L.K., Damasceno, B.S., Carvalho, M.N., Oliveira, E.H.C., Ghislandi, M.G., 2020. Adsorption capacity comparison between graphene oxide and graphene nanoplatelets for the removal of coloured textile dyes from wastewater. Environ. Technol. 41, 2360–2371.
de Menezes, F.D., Alencar, L.M.R., dos Santos, C.C., da Silva, M.I.B., Santos-Oliveira, R., 2020. Using graphene quantum dots for treating radioactive liquid waste. Environ. Sci. Pollut. Res. 27, 3508–3512.
Degueldre, C., 2017. Uranium as a renewable for nuclear energy. Prog. Nucl. Energy 94, 174–186.
Ding, J., Yan, Z., Feng, L., Zhai, F., Chen, X., Xu, Y., Tang, S., Huang, C., Li, L., Pan, N., He, Y., Jin, Y., Xia, C., 2019. Benzotriazole decorated graphene oxide for efficient removal of U(VI). Environ. Pollut. 253, 221–230.
Dubin, S., Gilje, S., Wang, K., Tung, V.C., Cha, K., Hall, A.S., Farrar, J., Varshneya, R., Yang, Y., Kaner, R.B., 2010. A One-Step, Solvothermal Reduction Method for Producing Reduced Graphene Oxide Dispersions in Organic Solvents. ACS Nano 4, 3845–3852.
Dutta, R.K., Shaida, M.A., Singla, K., Das, D., 2019. Highly efficient adsorptive removal of uranyl ions by a novel graphene oxide reduced by adenosine 5′-monophosphate (RGO-AMP). J. Mater. Chem. A 7, 664–678.
Eigler, S., Hirsch, A., 2014. Chemistry with Graphene and Graphene Oxide—Challenges for Synthetic Chemists. Angew. Chem. Int. Ed. 53, 7720–7738.
El-Maghrabi, H.H., Abdelmaged, S.M., Nada, A.A., Zahran, F., El-Wahab, S.A., Yahea, D., Hussein, G.M., Atrees, M.S., 2017. Magnetic graphene based nanocomposite for uranium scavenging. J. Hazard. Mater. 322, 370–379.
El-Magied, M.O.A., Mohammaden, T.F., El-Aassy, I.K., Gad, H.M.H., Hassan, A.M., Mahmoud, M.A., 2017. Decontamination of Uranium-Polluted Groundwater by Chemically-Enhanced. Sawdust-Activated Carbon, Colloids and Interfaces, p. 1.
Ersan, G., Apul, O.G., Perreault, F., Karanfil, T., 2017. Adsorption of organic contaminants by graphene nanosheets: A review. Water Res. 126, 385–398.
Fan, X., Xu, H., Zuo, S., Liang, Z., Yang, S., Chen, Y., 2020. Preparation and supercapacitive properties of phosphorus-doped reduced graphene oxide hydrogel. Electrochim. Acta 330, 135207.
Fang, S., Lin, Y., Hu, Y.H., 2019. Recent Advances in Green, Safe, and Fast Production of Graphene Oxide via Electrochemical Approaches. ACS Sustainable Chem. Eng. 7, 12671–12681.
Gado, M., Atia, B., Morcy, A., 2019. The role of graphene oxide anchored 1-amino-2-naphthol-4-sulphonic acid on the adsorption of uranyl ions from aqueous solution: kinetic and thermodynamic features. Int. J. Environ. Anal. Chem. 99, 996–1015.
Gao, M., Zhu, G., Gao, C., 2014. A review: adsorption materials for the removal and recovery of uranium from aqueous solutions. Energy and Environment Focus 3, 219–226.
Georgakilas, V., Otyepka, M., Bourlinos, A.B., Chandra, V., Kim, N., Kemp, K.C., Hobza, P., Zboril, R., Kim, K.S., 2012. Functionalization of Graphene: Covalent and Non-Covalent Approaches, Derivatives and Applications. Chem. Rev. 112, 6156–6214.
Ghasemi Torkabad, M., Keshtkar, A.R., Safdari, S.J., 2017. Uranium membrane separation from binary aqueous solutions of UO22+-K+ and UO22+-Ca2+ by the nanofiltration process. Sep. Sci. Technol. 52, 1095–1105.
Gopinath, K.P., Vo, D.-V.-N., Gnana Prakash, D., Adithya Joseph, A., Viswanathan, S., Arun, J., 2021. Environmental applications of carbon-based materials: a review. Environ. Chem. Lett. 19, 557–582.
Gunathilake, C., Górka, J., Dai, S., Jaroniec, M., 2015. Amidoxime-modified mesoporous silica for uranium adsorption under seawater conditions. J. Mater. Chem. A 3, 11650–11659.
Guo, H., Mei, P., Xiao, J., Huang, X., Ishag, A., Sun, Y., 2021. Carbon materials for extraction of uranium from seawater. Chemosphere 278, 130411.
Guo, X., Chen, R., Liu, Q., Liu, J., Zhang, H., Yu, J., Li, R., Zhang, M., Wang, J., 2019. Graphene Oxide and Silver Ions Coassisted Zeolitic Imidazolate Framework for Antifouling and Uranium Enrichment from Seawater. ACS Sustainable Chem. Eng. 7, 6185–6195.
Guo, X., Yang, H., Liu, Q., Liu, J., Chen, R., Zhang, H., Yu, J., Zhang, M., Li, R., Wang, J., 2020. A chitosan-graphene oxide/ZIF foam with anti-biofouling ability for uranium recovery from seawater. Chem. Eng. J. 382, 122850.
Gupta, D.K., Walther, C., 2020. Uranium in Plants and the Environment. Springer.
Haixia, X., de Barros, A.O.d.S., Sozzi-Guo, F., Müller, C., Gemini-Piperni, S., Alencar, L. M.R., Maia, F.F., Freire, V.N., de Menezes, F.D., Aran, V., 2021. Graphene: Insights on Biological, Radiochemical and Ecotoxicological Aspects. J. Biomed. Nanotechnol. 17, 131–148.
Han, B., Zhang, E., Cheng, G., 2018. Facile Preparation of Graphene Oxide-MIL-101 (Fe) Composite for the Efficient Capture of Uranium. Appl. Sci. 8, 2270.
Hu, B., Guo, X., Zheng, C., Song, G., Chen, D., Zhu, Y., Song, X., Sun, Y., 2019. Plasma-enhanced amidoxime/magnetic graphene oxide for efficient enrichment of U(VI) investigated by EXAFS and modeling techniques. Chem. Eng. J. 357, 66–74.
Hu, R., Shao, D., Wang, X., 2014. Graphene oxide/polypyrrole composites for highly selective enrichment of U (VI) from aqueous solutions. Polym. Chem. 5, 6207–6215.
Hu, T., Ding, S., Deng, H., 2016. Application of three surface complexation models on U (VI) adsorption onto graphene oxide. Chem. Eng. J. 289, 270–276.
Hu, X., Wang, Y., Wu, P., Li, Y., Tu, H., Wang, C., Yuan, D., Liu, Y., Cao, X., Liu, Z., 2020. Preparation of graphene/graphene nanoribbons hybrid aerogel and its application for the removal of uranium from aqueous solutions. J. Radioanal. Nucl. Chem. 325, 207–215.
Huang, Z.-W., Li, Z.-J., Wu, Q.-Y., Zheng, L.-R., Zhou, L.-M., Chai, Z.-F., Wang, X.-L., Shi, W.-Q., 2018. Simultaneous elimination of cationic uranium(vi) and anionic rhenium(vii) by graphene oxide–poly(ethyleneimine) macrostructures: a batch, XPS, EXAFS, and DFT combined study. Environ. Sci. Nano 5, 2077–2087.
Huang, Z., Li, Z., Zheng, L., Zhou, L., Chai, Z., Wang, X., Shi, W., 2017. Interaction mechanism of uranium(VI) with three-dimensional graphene oxide-chitosan composite: Insights from batch experiments, IR, XPS, and EXAFS spectroscopy. Chem. Eng. J. 328, 1066–1074.
Hummers Jr, W.S., Offeman, R.E., 1958. Preparation of graphitic oxide. Journal of the american chemical society 80, 1339–1339.
Huynh, M., Ozel, T., Liu, C., Lau, E.C., Nocera, D.G., 2017. Design of template-stabilized active and earth-abundant oxygen evolution catalysts in acid. Chem. Sci. 8, 4779–4794.
Jo, Y., Lee, J.-Y., Yun, J.-I., 2018. Adsorption of uranyl tricarbonate and calcium uranyl carbonate onto γ-alumina. Appl. Geochem. 94, 28–34.
Kasprzak, A., Zuchowska, A., Poplawska, M., 2018. Functionalization of graphene: does the organic chemistry matter? Beilstein journal of organic chemistry 14.
Kato, M., Azimi, M.D., Fayaz, S.H., Shah, M.D., Hoque, M.Z., Hamajima, N., Ohnuma, S., Ohtsuka, T., Maeda, M., Yoshinaga, M., 2016. Uranium in well drinking water of Kabul, Afghanistan and its effective, low-cost depuration using Mg-Fe based hydrotalcite-like compounds. Chemosphere 165, 27–32.
Katsoyiannis, I.A., Zouboulis, A.I., 2013. Removal of uranium from contaminated drinking water: a mini review of available treatment methods. Desalin. Water Treat. 51, 2915–2925.
Khan, S., Achazhiyath Edathil, A., Banat, F., 2019. Sustainable synthesis of graphene-based adsorbent using date syrup. Sci. Rep. 9, 18106.
Kim, H., Kang, S.-O., Park, S., Park, H.S., 2015. Adsorption isotherms and kinetics of cationic and anionic dyes on three-dimensional reduced graphene oxide macrostructure. J. Ind. Eng. Chem. 21, 1191–1196.
Konkena, B., Vasudevan, S., 2012. Understanding Aqueous Dispersibility of Graphene Oxide and Reduced Graphene Oxide through pKa Measurements. J. Phys. Chem. Lett. 3, 867–872.
Krachler, M., Varga, Z., Nicholl, A., Mayer, K., 2019. Analytical considerations in the determination of uranium isotope ratios in solid uranium materials using laser ablation multi-collector ICP-MS. Analytica Chimica Acta: X 2, 100018.
Kumar, A., Khandelwal, M., 2014. Amino acid mediated functionalization and reduction of graphene oxide – synthesis and the formation mechanism of nitrogen-doped graphene. New J. Chem. 38, 3457–3467.
Kumar, N., Srivastava, V.C., 2018. Simple Synthesis of Large Graphene Oxide Sheets via Electrochemical Method Coupled with Oxidation Process. ACS Omega 3, 10233–10242.
Kumar, N., Srivastava, V.C., 2021. Dimethyl carbonate production via transesterification reaction using nitrogen functionalized graphene oxide nanosheets. Renewable Energy.
Kumar, V., Kim, K.-H., Park, J.-W., Hong, J., Kumar, S., 2017. Graphene and its nanocomposites as a platform for environmental applications. Chem. Eng. J. 315, 210–232.
Lai, K.C., Lee, L.Y., Hiew, B.Y.Z., Thangalazhy-Gopakumar, S., Gan, S., 2019. Environmental application of three-dimensional graphene materials as adsorbents for dyes and heavy metals: Review on ice-templating method and adsorption mechanisms. J. Environ. Sci. 79, 174–199.
Lei, H., Zhou, D., Tang, J., Hu, X., Pan, N., Zou, H., Chi, F., Wang, X., 2020. Epoxy graphene oxide from a simple photo-Fenton reaction and its hybrid with phytic acid for enhancing U(VI) capture. Sci. Total Environ. 738, 140316.
Li, J., Qin, W., Xie, J., Lei, H., Zhu, Y., Huang, W., Xu, X., Zhao, Z., Mai, W., 2018. Sulphur-doped reduced graphene oxide sponges as high-performance free-standing anodes for K-ion storage. Nano Energy 53, 415–424.
Li, L., Wu, H., Chen, J., Xu, L., Sheng, G., Fang, P., Du, K., Shen, C., Guo, X., 2021a. Anchoring nanoscale iron sulfide onto graphene oxide for the highly efficient immobilization of uranium (VI) from aqueous solutions. J. Mol. Liq. 332, 115910.
Li, S., Yang, P., Liu, X., Zhang, J., Xie, W., Wang, C., Liu, C., Guo, Z., 2019. Graphene oxide based dopamine mussel-like cross-linked polyethylene imine nanocomposite coating with enhanced hexavalent uranium adsorption. J. Mater. Chem. A 7, 16902–16911.
Li, Y., He, H., Liu, Z., Lai, Z., Wang, Y., 2021b. A facile method for preparing three-dimensional graphene nanoribbons aerogel for uranium(VI) and thorium(IV) adsorption. J. Radioanal. Nucl. Chem. 328, 289–298.
Li, Z.-J., Huang, Z.-W., Guo, W.-L., Wang, L., Zheng, L.-R., Chai, Z.-F., Shi, W.-Q., 2017. Enhanced Photocatalytic Removal of Uranium(VI) from Aqueous Solution by Magnetic TiO2/Fe3O4 and Its Graphene Composite. Environ. Sci. Technol. 51, 5666–5674.
Li, Z., Chen, F., Yuan, L., Liu, Y., Zhao, Y., Chai, Z., Shi, W., 2012. Uranium(VI) adsorption on graphene oxide nanosheets from aqueous solutions. Chem. Eng. J. 210, 539–546.

Liao, Y., Wang, M., Chen, D., 2018. Preparation of polydopamine-modified graphene oxide/chitosan aerogel for uranium (VI) adsorption. Ind. Eng. Chem. Res. 57, 8472–8483.
Liao, Y., Wang, M., Chen, D., 2019. Electrosorption of uranium(VI) by highly porous phosphate-functionalized graphene hydrogel. Appl. Surf. Sci. 484, 83–96.
Lin, Y.-W., 2020. Uranyl Binding to Proteins and Structural-Functional Impacts. Biomolecules 10.
Lingamdinne, L.P., Choi, Y.-L., Kim, I.-S., Yang, J.-K., Koduru, J.R., Chang, Y.-Y., 2017. Preparation and characterization of porous reduced graphene oxide based inverse spinel nickel ferrite nanocomposite for adsorption removal of radionuclides. J. Hazard. Mater. 326, 145–156.
Liu, D., Liu, Z., Wang, C., Lai, Y., 2016a. Removal of uranium(VI) from aqueous solution using nanoscale zero-valent iron supported on activated charcoal. J. Radioanal. Nucl. Chem. 310, 1131–1137.
Liu, H., Mao, Y., 2021. Graphene Oxide-based Nanomaterials for Uranium Adsorptive Uptake. ES Mater. Manuf. 13, 3–22.
Liu, H., Xie, S., Liao, J., Yan, T., Liu, Y., Tang, X., 2018a. Novel graphene oxide/bentonite composite for uranium (VI) adsorption from aqueous solution. J. Radioanal. Nucl. Chem. 317, 1349–1360.
Liu, J., Yang, H., Zhen, S.G., Poh, C.K., Chaurasia, A., Luo, J., Wu, X., Yeow, E.K.L., Sahoo, N.G., Lin, J., Shen, Z., 2013. A green approach to the synthesis of high-quality graphene oxide flakes via electrochemical exfoliation of pencil core. RSC Adv. 3, 11745–11750.
Liu, S., Li, S., Zhang, H., Wu, L., Sun, L., Ma, J., 2016b. Removal of uranium (VI) from aqueous solution using graphene oxide and its amine-functionalized composite. J. Radioanal. Nucl. Chem. 309, 607–614.
Liu, S., Ma, J., Zhang, W., Luo, F., Luo, M., Li, F., Wu, L., 2015a. Three-dimensional graphene oxide/phytic acid composite for uranium (VI) sorption. J. Radioanal. Nucl. Chem. 306, 507–514.
Liu, S., Ouyang, J., Luo, J., Sun, L., Huang, G., Ma, J., 2018b. Removal of uranium (VI) from aqueous solution using graphene oxide functionalized with diethylenetriaminepentaacetic phenylenediamine. J. Nucl. Sci. Technol. 55, 781–791.
Liu, S., Zhang, H., Peng, D., Yuan, D., Wu, L., Ma, J., 2017. Uranium uptake with graphene oxide sponge prepared by facile EDTA-assisted hydrothermal process. Int. J. Energy Res. 41, 263–273.
Liu, X., Li, J., Wang, X., Chen, C., Wang, X., 2015b. High performance of phosphate-functionalized graphene oxide for the selective adsorption of U(VI) from acidic solution. J. Nucl. Mater. 466, 56–64.
Ma, J., Zhao, Q., Zhou, L., Wen, T., Wang, J., 2019. Mutual effects of U(VI) and Eu(III) immobilization on interpenetrating 3-dimensional MnO2/graphene oxide composites. Sci. Total Environ. 695, 133696.
Magne, T.M., de Oliveira Vieira, T., Costa, B., Alencar, L.M.R., Ricci-Junior, E., Hu, R., Qu, J., Zamora-Ledezma, C., Alexis, F., Santos-Oliveira, R., 2021. Factors affecting the biological response of Graphene. Colloids Surf., B 203, 111767.
Mahmoud, M.E., Fekry, N.A., Abdelfattah, A.M., 2020. Removal of uranium (VI) from water by the action of microwave-rapid green synthesized carbon quantum dots from starch-water system and supported onto polymeric matrix. J. Hazard. Mater. 397, 122770.
Marcano, D.C., Kosynkin, D.V., Berlin, J.M., Sinitskii, A., Sun, Z., Slesarev, A., Alemany, L.B., Lu, W., Tour, J.M., 2010. Improved Synthesis of Graphene Oxide. ACS Nano 4, 4806–4814.
Meng, H., Li, Z., Ma, F., Wang, X., Zhou, W., Zhang, L., 2015. Synthesis and characterization of surface ion-imprinted polymer based on SiO 2-coated graphene oxide for selective adsorption of uranium (vi). RSC Adv. 5, 67662–67668.
Mohamud, H., Ivanov, P., Russell, B.C., Regan, P.H., Ward, N.I., 2018. Selective sorption of uranium from aqueous solution by graphene oxide-modified materials. J. Radioanal. Nucl. Chem. 316, 839–848.
Moraes, M.L.B.d., Ladeira, A.C.Q., 2021. The role of iron in the rare earth elements and uranium scavenging by Fe–Al-precipitates in acid mine drainage. Chemosphere 277, 130131.
Nasrollahzadeh, M., Babaei, F., Fakhri, P., Jaleh, B., 2015. Synthesis, characterization, structural, optical properties and catalytic activity of reduced graphene oxide/copper nanocomposites. RSC Adv. 5, 10782–10789.
Nezhad, M.M., Semnani, A., Tavakkoli, N., Shirani, M., 2021. Selective and highly efficient removal of uranium from radioactive effluents by activated carbon functionalized with 2-aminobenzoic acid as a new sorbent. J. Environ. Manage. 299, 113587.
Niu, F., Tao, L.-M., Deng, Y.-C., Wang, Q.-H., Song, W.-G., 2014. Phosphorus doped graphene nanosheets for room temperature NH3 sensing. New J. Chem. 38, 2269–2272.
Pal, P., 2017. Chapter 4 - Physicochemical Treatment Technology. In: Pal, P. (Ed.), Industrial Water Treatment Process Technology. Butterworth-Heinemann, pp. 145–171.
Pan, N., Li, L., Ding, J., Li, S., Wang, R., Jin, Y., Wang, X., Xia, C., 2016. Preparation of graphene oxide-manganese dioxide for highly efficient adsorption and separation of Th(IV)/U(VI). J. Hazard. Mater. 309, 107–115.
Park, S., An, J., Jung, I., Piner, R.D., An, S.J., Li, X., Velamakanni, A., Ruoff, R.S., 2009. Colloidal Suspensions of Highly Reduced Graphene Oxide in a Wide Variety of Organic Solvents. Nano Lett. 9, 1593–1597.
Park, S., Hu, Y., Hwang, J.O., Lee, E.-S., Casabianca, L.B., Cai, W., Potts, J.R., Ha, H.-W., Chen, S., Oh, J., Kim, S.O., Kim, Y.-H., Ishii, Y., Ruoff, R.S., 2012. Chemical structures of hydrazine-treated graphene oxide and generation of aromatic nitrogen doping. Nat. Commun. 3, 638.
Payne, T.E., Brendler, V., Ochs, M., Baeyens, B., Brown, P.L., Davis, J.A., Ekberg, C., Kulik, D.A., Lutzenkirchen, J., Missana, T., Tachi, Y., Van Loon, L.R., Altmann, S., 2013. Guidelines for thermodynamic sorption modelling in the context of radioactive waste disposal. Environ. Modell. Software 42, 143–156.
Pei, S., Cheng, H.-M., 2012. The reduction of graphene oxide. Carbon 50, 3210–3228.
Pei, S., Wei, Q., Huang, K., Cheng, H.-M., Ren, W., 2018. Green synthesis of graphene oxide by seconds timescale water electrolytic oxidation. Nat. Commun. 9, 145.
Peng, W., Huang, G., Yang, S., Guo, C., Shi, J., 2019. Performance of biopolymer/graphene oxide gels for the effective adsorption of U(VI) from aqueous solution. J. Radioanal. Nucl. Chem. 322, 861–868.
Peng, W., Li, H., Liu, Y., Song, S., 2017. A review on heavy metal ions adsorption from water by graphene oxide and its composites. J. Mol. Liq. 230, 496–504.
Pérez-Ramírez, E.E., de la Luz-Asunción, M., Martínez-Hernández, A.L., Velasco-Santos, C., 2016. Graphene materials to remove organic pollutants and heavy metals from water: photocatalysis and adsorption. Semiconductor Photocatalysis-Materials, Mechanisms and Applications. IntechOpen.
Pikula, K., Zakharenko, A., Chaika, V., Vedyagin, A., Orlova, T.Y., Mishakov, I., Kuznetsov, V., Park, S., Renieri, E., Kahru, A., 2018. Effects of carbon and silicon nanotubes and carbon nanofibers on marine microalgae Heterosigma akashiwo. Environ. Res. 166, 473–480.
Qian, Y., Yuan, Y., Wang, H., Liu, H., Zhang, J., Shi, S., Guo, Z., Wang, N., 2018. Highly efficient uranium adsorption by salicylaldoxime/polydopamine graphene oxide nanocomposites. J. Mater. Chem. A 6, 24676–24685.
Qiu, P., Wang, S., Tian, C., Lin, Z., 2019. Adsorption of low-concentration mercury in water by 3D cyclodextrin/graphene composites: Synergistic effect and enhancement mechanism. Environ. Pollut. 252, 1133–1141.
Ren, X., Li, J., Tan, X., Wang, X., 2013. Comparative study of graphene oxide, activated carbon and carbon nanotubes as adsorbents for copper decontamination. Dalton Trans. 42, 5266–5274.
Romanchuk, A.Y., Slesarev, A.S., Kalmykov, S.N., Kosynkin, D.V., Tour, J.M., 2013. Graphene oxide for effective radionuclide removal. PCCP 15, 2321–2327.
Rosen, M.R., Burow, K.R., Fram, M.S., 2019. Anthropogenic and geologic causes of anomalously high uranium concentrations in groundwater used for drinking water supply in the southeastern San Joaquin Valley. CA. Journal of Hydrology 577, 124009.
Saleem, H., Haneef, M., Abbasi, H.Y., 2018. Synthesis route of reduced graphene oxide via thermal reduction of chemically exfoliated graphene oxide. Mater. Chem. Phys. 204, 1–7.
Sar, S.K., Diwan, V., Biswas, S., Singh, S., Sahu, M., Jindal, M.K., Arora, A., 2018. Study of uranium level in groundwater of Balod district of Chhattisgarh state, India and assessment of health risk. Hum. Ecolog. Risk Assessment Int. J. 24, 691–698.
Seo, M., Yoon, D., Hwang, K.S., Kang, J.W., Kim, J., 2013. Supercritical alcohols as solvents and reducing agents for the synthesis of reduced graphene oxide. Carbon 64, 207–218.
Shao, L., Wang, X., Ren, Y., Wang, S., Zhong, J., Chu, M., Tang, H., Luo, L., Xie, D., 2016. Facile fabrication of magnetic cucurbit [6] uril/graphene oxide composite and application for uranium removal. Chem. Eng. J. 286, 311–319.
Shao, L., Zhong, J., Ren, Y., Tang, H., Wang, X., 2017. Perhydroxy-CB [6] decorated graphene oxide composite for uranium (VI) removal. J. Radioanal. Nucl. Chem. 311, 627–635.
Singhal, P., Vats, B.G., Yadav, A., Pulhani, V., 2020. Efficient extraction of uranium from environmental samples using phosphoramide functionalized magnetic nanoparticles: Understanding adsorption and binding mechanisms. J. Hazard. Mater. 384, 121353.
Song, S., Wang, K., Zhang, Y., Wang, Y., Zhang, C., Wang, X., Zhang, R., Chen, J., Wen, T., Wang, X., 2019. Self-assembly of graphene oxide/PEDOT:PSS nanocomposite as a novel adsorbent for uranium immobilization from wastewater. Environ. Pollut. 250, 196–205.
Song, W., Shao, D., Lu, S., Wang, X., 2014. Simultaneous removal of uranium and humic acid by cyclodextrin modified graphene oxide nanosheets. Sci. China Chem. 57, 1291–1299.
Song, X., Tan, L., Sun, X., Ma, H., Zhu, L., Yi, X., Dong, Q., Gao, J., 2016. Facile preparation of NiCo2O4@rGO composites for the removal of uranium ions from aqueous solutions. Dalton Trans. 45, 16931–16937.
Strawn, D.G., 2021. Sorption Mechanisms of Chemicals in Soils. Soil Syst. 5.
Su, M., Liu, Z., Wu, Y., Peng, H., Ou, T., Huang, S., Song, G., Kong, L., Chen, N., Chen, D., 2021. Graphene oxide functionalized with nano hydroxyapatite for the efficient removal of U(VI) from aqueous solution. Environ. Pollut. 268, 115786.
Sun, Y., Shao, D., Chen, C., Yang, S., Wang, X., 2013. Highly efficient enrichment of radionuclides on graphene oxide-supported polyaniline. Environ. Sci. Technol. 47, 9904–9910.
Sun, Y., Wang, X., Ai, Y., Yu, Z., Huang, W., Chen, C., Hayat, T., Alsaedi, A., Wang, X., 2017. Interaction of sulfonated graphene oxide with U (VI) studied by spectroscopic analysis and theoretical calculations. Chem. Eng. J. 310, 292–299.
Sun, Y., Yang, S., Chen, Y., Ding, C., Cheng, W., Wang, X., 2015a. Adsorption and desorption of U (VI) on functionalized graphene oxides: a combined experimental and theoretical study. Environ. Sci. Technol. 49, 4255–4262.
Sun, Y., Yang, S., Chen, Y., Ding, C., Cheng, W., Wang, X., 2015b. Adsorption and Desorption of U(VI) on Functionalized Graphene Oxides: A Combined Experimental and Theoretical Study. Environ. Sci. Technol. 49, 4255–4262.
Tan, L., Liu, Q., Song, D., Jing, X., Liu, J., Li, R., Hu, S., Liu, L., Wang, J., 2015a. Uranium extraction using a magnetic CoFe2O4–graphene nanocomposite: kinetics and thermodynamics studies. New J. Chem. 39, 2832–2838.
Tan, L., Wang, J., Liu, Q., Sun, Y., Jing, X., Liu, L., Liu, J., Song, D., 2015b. The synthesis of a manganese dioxide–iron oxide–graphene magnetic nanocomposite for enhanced uranium(vi) removal. New J. Chem. 39, 868–876.
Tan, L., Wang, Y., Liu, Q., Wang, J., Jing, X., Liu, L., Liu, J., Song, D., 2015c. Enhanced adsorption of uranium (VI) using a three-dimensional layered double hydroxide/graphene hybrid material. Chem. Eng. J. 259, 752–760.

Tatarchuk, T., Shyichuk, A., Mironyuk, I., Naushad, M., 2019. A review on removal of uranium(VI) ions using titanium dioxide based sorbents. J. Mol. Liq. 293, 111563.
Tu, N.D.K., Choi, J., Park, C.R., Kim, H., 2015. Remarkable Conversion Between n- and p-Type Reduced Graphene Oxide on Varying the Thermal Annealing Temperature. Chem. Mater. 27, 7362–7369.
Upadhyay, R.K., Soin, N., Roy, S.S., 2014. Role of graphene/metal oxide composites as photocatalysts, adsorbents and disinfectants in water treatment: a review. RSC Adv. 4, 3823–3851.
Valeur, E., Bradley, M., 2009. Amide bond formation: beyond the myth of coupling reagents. Chem. Soc. Rev. 38, 606–631.
Verma, S., Dutta, R.K., 2015. A facile method of synthesizing ammonia modified graphene oxide for efficient removal of uranyl ions from aqueous medium. RSC Adv. 5, 77192–77203.
Verma, S., Dutta, R.K., 2017. Development of cysteine amide reduced graphene oxide (CARGO) nano-adsorbents for enhanced uranyl ions removal from aqueous medium. J. Environ. Chem. Eng. 5, 4547–4558.
Verma, S., Dutta, R.K., 2020. Adsorptive Removal of Toxic Dyes Using Chitosan and Its Composites. In: Naushad, M., Lichtfouse, E. (Eds.), Green Materials for Wastewater Treatment. Springer International Publishing, Cham, pp. 223–255.
Vikrant, K., Kim, K.-H., 2019. Nanomaterials for the adsorptive treatment of Hg(II) ions from water. Chem. Eng. J. 358, 264–282.
Wang, C.L., Li, Y., Liu, C.L., 2015a. Sorption of uranium from aqueous solutions with graphene oxide. J. Radioanal. Nucl. Chem. 304, 1017–1025.
Wang, F., Li, H., Liu, Q., Li, Z., Li, R., Zhang, H., Liu, L., Emelchenko, G.A., Wang, J., 2016a. A graphene oxide/amidoxime hydrogel for enhanced uranium capture. Sci. Rep. 6, 19367.
Wang, J., Fang, F., Zhou, Y., Yin, M., Liu, J., Wang, J., Wu, Y., Beiyuan, J., Chen, D., 2020a. Facile modification of graphene oxide and its application for the aqueous uranyl ion sequestration: Insights on the mechanism. Chemosphere 258, 127152.
Wang, L., Li, Z., Wu, Q., Huang, Z., Yuan, L., Chai, Z., Shi, W., 2020b. Layered structure-based materials: challenges and opportunities for radionuclide sequestration. Environ. Sci. Nano 7, 724–752.
Wang, L., Song, H., Yuan, L., Li, Z., Zhang, Y., Gibson, J.K., Zheng, L., Chai, Z., Shi, W., 2018a. Efficient U(VI) Reduction and Sequestration by Ti2CTx MXene. Environ. Sci. Technol. 52, 10748–10756.
Wang, X., Chen, Z., Wang, X., 2015b. Graphene oxides for simultaneous highly efficient removal of trace level radionuclides from aqueous solutions. Sci. China Chem. 58, 1766–1773.
Wang, X., Liu, Q., Liu, J., Chen, R., Zhang, H., Li, R., Li, Z., Wang, J., 2017. 3D self-assembly polyethyleneimine modified graphene oxide hydrogel for the extraction of uranium from aqueous solution. Appl. Surf. Sci. 426, 1063–1074.
Wang, X., Yu, S., Jin, J., Wang, H., Alharbi, N.S., Alsaedi, A., Hayat, T., Wang, X., 2016b. Application of graphene oxides and graphene oxide-based nanomaterials in radionuclide removal from aqueous solutions. Sci. Bull. 61, 1583–1593.
Wang, Y., Hu, X., Liu, Y., Li, Y., Lan, T., Wang, C., Liu, Y., Yuan, D., Cao, X., He, H., Zhou, L., Liu, Z., Chew, J.W., 2021a. Assembly of three-dimensional ultralight poly (amidoxime)/graphene oxide nanoribbons aerogel for efficient removal of uranium (VI) from water samples. Sci. Total Environ. 765, 142686.
Wang, Y., Lin, Z., Zhang, H., Liu, Q., Yu, J., Liu, J., Chen, R., Zhu, J., Wang, J., 2021b. Anti-bacterial and super-hydrophilic bamboo charcoal with amidoxime modified for efficient and selective uranium extraction from seawater. J. Colloid Interface Sci. 598, 455–463.
Wang, Y., Wang, Z., Ang, R., Yang, J., Liu, N., Liao, J., Yang, Y., Tang, J., 2015c. Synthesis of amidoximated graphene oxide nanoribbons from unzipping of multiwalled carbon nanotubes for selective separation of uranium(vi). RSC Adv. 5, 89309–89318.
Wang, Z., Luo, C., Zhang, Y., Gong, Y., Wu, J., Fu, Q., Pan, C., 2018b. Construction of hierarchical TiO2 nanorod array/graphene/ZnO nanocomposites for high-performance photocatalysis. J. Mater. Sci. 53, 15376–15389.
Wang, Z., Wang, Y., Liao, J., Yang, Y., Liu, N., Tang, J., 2016c. Improving the adsorption ability of graphene sheets to uranium through chemical oxidation, electrolysis and ball-milling. J. Radioanal. Nucl. Chem. 308, 1095–1102.
Wen, R., Li, Y., Zhang, M., Guo, X., Li, X., Li, X., Han, J., Hu, S., Tan, W., Ma, L., 2018. Graphene-synergized 2D covalent organic framework for adsorption: a mutual promotion strategy to achieve stabilization and functionalization simultaneously. J. Hazard. Mater. 358, 273–285.
Winde, F., Erasmus, E., Geipel, G., 2017. Uranium contaminated drinking water linked to leukaemia—Revisiting a case study from South Africa taking alternative exposure pathways into account. Sci. Total Environ. 574, 400–421.
Wu, D., Wang, T., Wang, L., Jia, D., 2019. Hydrothermal synthesis of nitrogen, sulfur co-doped graphene and its high performance in supercapacitor and oxygen reduction reaction. Microporous Mesoporous Mater. 290, 109556.
Wu, J., Tian, K., Wang, J., 2018. Adsorption of uranium (VI) by amidoxime modified multiwalled carbon nanotubes. Prog. Nucl. Energy 106, 79–86.
Wu, W., Yang, Y., Zhou, H., Ye, T., Huang, Z., Liu, R., Kuang, Y., 2013. Highly efficient removal of Cu (II) from aqueous solution by using graphene oxide. Water Air Soil Pollut. 224, 1–8.
Wua, L.-L., Caoc, Y.-S., Lia, Z.-P., Hua, L., Zhanga, Z.-J., Yua, Q., 2020. Preparation of areca residue activated carbon composite and its adsorption performance for uranium (VI) in wastewater. Desalination and Water Treatment 182, 144–154.
Xiao, J., Lv, W., Xie, Z., Tan, Y., Song, Y., Zheng, Q., 2016. Environmentally friendly reduced graphene oxide as a broad-spectrum adsorbent for anionic and cationic dyes via π–π interactions. J. Mater. Chem. A 4, 12126–12135.
Yang, A., Wang, Z., Zhu, Y., 2021a. Facile preparation and highly efficient sorption of magnetic composite graphene oxide/Fe3O4/GC for uranium removal. Sci. Rep. 11, 8440.
Yang, A., Zhu, Y., Huang, C.P., 2018. Facile preparation and adsorption performance of graphene oxide-manganese oxide composite for uranium. Sci. Rep. 8, 9058.
Yang, A., Zhu, Y., Li, P., Huang, C.P., 2019a. Preparation of a magnetic reduced-graphene oxide/tea waste composite for high-efficiency sorption of uranium. Sci. Rep. 9, 6471.
Yang, P., Li, S., Liu, C., Shen, C., Liu, X., 2021b. Water-endurable intercalated graphene oxide adsorbent with highly efficient uranium capture from acidic wastewater. Sep. Purif. Technol. 263, 118364.
Yang, P., Liu, Q., Liu, J., Zhang, H., Li, Z., Li, R., Liu, L., Wang, J., 2017. Bovine Serum Albumin-Coated Graphene Oxide for Effective Adsorption of Uranium(VI) from Aqueous Solutions. Ind. Eng. Chem. Res. 56, 3588–3598.
Yang, P., Zhang, H., Liu, Q., Liu, J., Chen, R., Yu, J., Hou, J., Bai, X., Wang, J., 2019b. Nano-sized architectural design of multi-activity graphene oxide (GO) by chemical post-decoration for efficient uranium(VI) extraction. J. Hazard. Mater. 375, 320–329.
Yang, S., Huang, Y., Huang, G., Peng, W., Guo, C., Shi, J., 2020. Preparation of amidoxime-functionalized biopolymer/graphene oxide gels and their application in selective adsorption separation of U (VI) from aqueous solution. J. Radioanal. Nucl. Chem. 1–9.
Yeh, T.-F., Chen, S.-J., Yeh, C.-S., Teng, H., 2013. Tuning the Electronic Structure of Graphite Oxide through Ammonia Treatment for Photocatalytic Generation of H2 and O2 from Water Splitting. J. Phys. Chem. C 117, 6516–6524.
Yi, X., Sun, F., Han, Z., Han, F., He, J., Ou, M., Gu, J., Xu, X., 2018. Graphene oxide encapsulated polyvinyl alcohol/sodium alginate hydrogel microspheres for Cu (II) and U (VI) removal. Ecotoxicol. Environ. Saf. 158, 309–318.
Yin, W., Zhan, X., Fang, P., Xia, M., Yu, J., Chi, R.-A., 2019. A Facile One-Pot Strategy to Functionalize Graphene Oxide with Poly(amino-phosphonic Acid) Derived from Wasted Acrylic Fibers for Effective Gd(III) Capture. ACS Sustain. Chem. Eng. 7, 19857–19869.
Yu, J.-G., Yu, L.-Y., Yang, H., Liu, Q., Chen, X.-H., Jiang, X.-Y., Chen, X.-Q., Jiao, F.-P., 2015. Graphene nanosheets as novel adsorbents in adsorption, preconcentration and removal of gases, organic compounds and metal ions. Sci. Total Environ. 502, 70–79.
Yu, S., Wei, D., Shi, L., Ai, Y., Zhang, P., Wang, X., 2019. Three-dimensional graphene/titanium dioxide composite for enhanced U(VI) capture: Insights from batch experiments, XPS spectroscopy and DFT calculation. Environ. Pollut. 251, 975–983.
Zhang, L., Li, Y., Guo, H., Zhang, H., Zhang, N., Hayat, T., Sun, Y., 2019a. Decontamination of U (VI) on graphene oxide/Al2O3 composites investigated by XRD, FT-IR and XPS techniques. Environ. Pollut. 248, 332–338.
Zhang, Q., Zhao, D., Ding, Y., Chen, Y., Li, F., Alsaedi, A., Hayat, T., Chen, C., 2019b. Synthesis of Fe–Ni/graphene oxide composite and its highly efficient removal of uranium(VI) from aqueous solution. J. Cleaner Prod. 230, 1305–1315.
Zhang, S., Yuan, D., Zhang, Q., Wang, Y., Liu, Y., Zhao, J., Chen, B., 2020. Highly efficient removal of uranium from highly acidic media achieved using a phosphine oxide and amino functionalized superparamagnetic composite polymer adsorbent. J. Mater. Chem. A 8, 10925–10934.
Zhang, Y., Zhao, H., Fan, Q., Zheng, X., Li, P., Liu, S., Wu, W., 2011. Sorption of U(VI) onto a decarbonated calcareous soil. J. Radioanal. Nucl. Chem. 288, 395–404.
Zhang, Z.-B., Qiu, Y.-F., Dai, Y., Wang, P.-F., Gao, B., Dong, Z.-M., Cao, X.-H., Liu, Y.-H., Le, Z.-G., 2016. Synthesis and application of sulfonated graphene oxide for the adsorption of uranium(VI) from aqueous solutions. J. Radioanal. Nucl. Chem. 310, 547–557.
Zhao, C., Liu, J., Yuan, G., Liu, J., Zhang, H., Yang, J., Yang, Y., Liu, N., Sun, Q., Liao, J., 2018. A novel activated sludge-graphene oxide composites for the removal of uranium (VI) from aqueous solutions. J. Mol. Liq. 271, 786–794.
Zhao, D., Wang, Y., Zhao, S., Wakeel, M., Wang, Z., Shaikh, R.S., Hayat, T., Chen, C., 2019. A simple method for preparing ultra-light graphene aerogel for rapid removal of U(VI) from aqueous solution. Environ. Pollut. 251, 547–554.
Zhao, G., Wen, T., Yang, X., Yang, S., Liao, J., Hu, J., Shao, D., Wang, X., 2012. Preconcentration of U (VI) ions on few-layered graphene oxide nanosheets from aqueous solutions. Dalton Trans. 41, 6182–6188.
Zhao, M., Tesfay Reda, A., Zhang, D., 2020. Reduced Graphene Oxide/ZIF-67 Aerogel Composite Material for Uranium Adsorption in Aqueous Solutions. ACS Omega 5, 8012–8022.
Zhao, Y., Li, J., Zhang, S., Chen, H., Shao, D., 2013. Efficient enrichment of uranium(vi) on amidoximated magnetite/graphene oxide composites. RSC Adv. 3, 18952–18959.
Zhao, Z., Li, J., Wen, T., Shen, C., Wang, X., Xu, A., 2015. Surface functionalization graphene oxide by polydopamine for high affinity of radionuclides. Colloids Surf., A 482, 258–266.
Zhu, J., Zhang, H., Liu, Q., Wang, C., Sun, Z., Li, R., Liu, P., Zhang, M., Wang, J., 2019a. Metal-organic frameworks (MIL-68) decorated graphene oxide for highly efficient enrichment of uranium. J. Taiwan Inst. Chem. Eng. 99, 45–52.
Zhu, W., Lei, J., Li, Y., Dai, L., Chen, T., Bai, X., Wang, L., Duan, T., 2019b. Procedural growth of fungal hyphae/Fe3O4/graphene oxide as ordered-structure composites for water purification. Chem. Eng. J. 355, 777–783.
Zong, P., Cao, D., Cheng, Y., Wang, S., Zhang, J., Guo, Z., Hayat, T., Alharbi, N.S., He, C., 2019. Carboxymethyl cellulose supported magnetic graphene oxide composites by plasma induced technique and their highly efficient removal of uranium ions. Cellulose 26, 4039–4060.
Zong, P., Wang, S., Zhao, Y., Wang, H., Pan, H., He, C., 2013. Synthesis and application of magnetic graphene/iron oxides composite for the removal of U(VI) from aqueous solutions. Chem. Eng. J. 220, 45–52.